C.P. No. 1332

C.P. No. 1332

PROCUREMENT EXECUTIVE, MINISTRY OF DEFENCE

AERONAUTICAL RESEARCH COUNCIL

CURRENT PAPERS

Interference Problems on Wing-Fuselage Combinations Part II Symmetrical Unswept Wing at Zero Incidence attached to a Cylindrical Fuselage at Zero Incidence in Midwing Position

by

J. Weber and M. G. Joyce

Aerodynamics Dept., R.A.E., Farnborough

LONDON: HER MAJESTY'S STATIONERY OFFICE

1975

PRICE £2-30 NET

UDC 533.695.12 : 533.693.2 : 533.6.048.2 : 533.6.011.32

CP No.1332*
August 1971

INTERFERENCE PROBLEMS ON WING-FUSELAGE COMBINATIONS PART II: SYMMETRICAL UNSWEPT WING AT ZERO INCIDENCE ATTACHED TO A CYLINDRICAL FUSELAGE AT ZERO INCIDENCE IN MIDWING POSITION

by

J. Weber

M. G. Joyce

SUMMARY

The incompressible flow field past a single straight infinitely long source line which crosses a circular cylindrical fuselage at right angles has been studied. In particular, the streamwise velocity component induced in the plane through the source line and the axis of the fuselage and the streamwise and circumferential velocity components induced on the surface of the fuselage have been determined numerically.

The results are used to determine the interference effect on the displacement flow past an unswept wing of infinite aspect ratio attached to a cylindrical fuselage. It is shown how the interference effect varies with the ratio R/c between the body radius and the wing chord.

---

* Replaces RAE Technical Report 71179 - ARC 33437

CONTENTS

1 INTRODUCTION

In this Report we intend to study some of the interference effects between a fuselage and a non-lifting wing of finite thickness. We choose a simple case, similar to the configuration studied in Part I [1], and consider an infinite cylindrical fuselage of circular cross section with the axis parallel to the main stream and an unswept wing of constant chord and infinite span with the same symmetrical section along the span. The fuselage is attached in mid-wing position.

The task is to determine the pressure distribution on this wing-fuselage combination in incompressible flow. The problem can be dealt with by the method of A.M.O. Smith (see e.g. Ref.3), which approximates such a configuration by a series of planar source panels of constant strength, situated on the surface of wing and fuselage. This method requires rather too much computational effort for preliminary studies of a series of configurations. We intend therefore to study the problem within the accuracy of a small perturbation theory and thus to represent the wing by a source distribution in the plane of the wing. We extend this source distribution inside the fuselage in such a way that the local reflection effect of the body wall is represented (see Ref.2). For the special case of an unswept wing, this means that we deal with an unswept gross wing of constant section, i.e. a chordwise distribution of straight infinite source lines of constant strength, which cross the fuselage at right angles.

The source distribution in the plane of the wing induces a non-zero normal velocity at the surface of the fuselage. To cancel this we add a further source distribution on the surface of the fuselage. This additional source distribution induces streamwise and spanwise velocity components in the wing plane and streamwise and circumferential velocity components on the surface of the fuselage.

We intend to study wings of different section shape and of different ratio between wing chord and body diameter. To reduce the amount of computation we consider first an isolated source line in the presence of the fuselage and determine the streamwise velocity component induced in the wing plane and on the surface of the fuselage. We determine also the circumferential velocity component on the fuselage, but we have not computed the spanwise velocity component in the wing plane since it vanishes at the line where the wing plane intersects the fuselage and is of little importance away from the fuselage.

To illustrate the importance of the interference effect on the displacement flow we have calculated some velocity distributions on a 10 per cent thick wing,

with RAE 101 section, attached to fuselages of different diameter. A first-order and a second-order theory have been considered.

2 A SINGLE STRAIGHT SOURCE LINE IN THE PRESENCE OF A CIRCULAR CYLINDRICAL FUSELAGE

2.1 Velocities induced by the source line

Let x, y, z be a Cartesian system of coordinates and x, r, θ a system of cylindrical coordinates. We consider an infinite straight source line through x = 0, z = 0, i.e. along the y-axis. The strength of the source line is constant and equal to Q per unit length. We consider further an infinitely long cylindrical fuselage of circular cross section $y^2 + z^2 = R^2 = 1$. The source line thus crosses the fuselage at right angles. In the following equations all lengths are made dimensionless with the radius R of the fuselage.

The velocity field of the source line has the components

$$v_x = \frac{Q}{2\pi} \frac{x}{x^2 + z^2}$$

$$v_y = 0$$

$$v_z = \frac{Q}{2\pi} \frac{z}{x^2 + z^2} \quad .$$

The source line therefore induces at the surface of the fuselage a normal velocity component (positive outwards):

$$v_{nQ}(x,\theta) = v_y \cos\theta + v_z \sin\theta$$

$$= \frac{Q}{2\pi} \frac{\sin^2\theta}{x^2 + \sin^2\theta} \quad . \qquad (1)$$

In the following, we shall require the mean value of the normal velocity at the cross section x = const

$$\bar{v}_{nQ}(x) = \frac{1}{2\pi} \int_0^{2\pi} v_{nQ}(x,\theta) d\theta \quad . \qquad (2)$$

It is

$$\bar{v}_{nQ}(x) = \frac{Q}{2\pi}\left[1 - \sqrt{\frac{x^2}{1+x^2}}\right]. \qquad (3)$$

The integral of $v_n(x,\theta)$ over the fuselage is

$$\int_{-\infty}^{\infty}\int_{0}^{2\pi} v_{nQ}(x,\theta)\,d\theta\,dx = 2\pi \int_{-\infty}^{\infty} \bar{v}_{nQ}(x)\,dx$$

$$= 2\pi \frac{Q}{2\pi}\, 2 \int_{0}^{\infty}\left[1 - \sqrt{\frac{x^2}{1+x^2}}\right] dx = 2Q \ ,$$

i.e. the integral is equal to the total source strength of that part of the source line which lies within the fuselage; as it should be.

The normal velocity induced by a source line differs in an essential way from the normal velocity induced by a straight vortex (see Fig.1 and Fig.1 of Ref.1). The normal velocity $v_{n\Gamma}(x,\theta)$ induced by a vortex is an anti-symmetrical function with respect to x and with respect to θ, whilst the $v_{nQ}(x,\theta)$ induced by a source line is a symmetrical function with respect to x and to θ. As a consequence the mean value $\bar{v}_{n\Gamma}(x)$ vanishes for each station x, whilst $\bar{v}_{nQ}(x)$ is non-zero. We note further that $v_{nQ}(x,\theta)$ decreases more rapidly with increasing x than $v_{n\Gamma}(x,\theta)$.

2.2 Strength of the source distribution on the fuselage which makes the fuselage a stream surface

As with the vortex crossing a fuselage, we intend to use a source distribution on the surface of the fuselage to cancel the normal velocity $v_{nQ}(x,\theta)$ induced by the source line. The strength of the source distribution $q(x,\theta)$ must satisfy the equation:

$$v_{nq}(x,\theta) = - v_{nQ}(x,\theta)$$

$$= \frac{q(x,\theta)}{2} + \int_{-\infty}^{\infty} \int_{0}^{2\pi} \frac{q(x',\theta')\,[1 - \cos(\theta - \theta')]\,d\theta'dx'}{4\pi \sqrt{(x - x')^2 + 2[1 - \cos(\theta - \theta')]}^3}$$

$$= \frac{q(x,\theta)}{2} + \int_{0}^{2\pi} \frac{q(x,\theta')}{4\pi}\, d\theta'$$

$$+ \int_{-\infty}^{\infty} \int_{0}^{2\pi} \frac{[q(x',\theta') - q(x,\theta')]\,[1 - \cos(\theta - \theta')]\,d\theta'dx'}{4\pi \sqrt{(x - x')^2 + 2[1 - \cos(\theta - \theta')]}^3} \quad . \qquad (4)$$

We intend to solve this equation only approximately by an iteration procedure. Equation (4) suggests as a first approximation the source distribution $q^{(0)}(x,\theta)$ obtained by neglecting the last term of this equation. Thus $q^{(0)}$ must satisfy the equation

$$q^{(0)}(x,\theta) + \bar{q}^{(0)}(x) = - 2v_{nQ}(x,\theta) \qquad (5)$$

where

$$\bar{q}^{(0)}(x) = \frac{1}{2\pi} \int_{0}^{2\pi} q^{(0)}(x,\theta)d\theta \quad . \qquad (6)$$

Taking the mean value with respect to θ of both sides of equation (5) we see at once that

$$\bar{q}^{(0)}(x) = - \bar{v}_{nQ}(x) \qquad (7)$$

and hence

$$q^{(0)}(x,\theta) = - 2v_{nQ}(x,\theta) + \bar{v}_{nQ}(x) \quad . \qquad (8)$$

The integral of the source strength $q^{(0)}(x,\theta)$ taken over the whole fuselage is

$$\int_{-\infty}^{\infty} \int_{0}^{2\pi} q^{(0)}(x,\theta)\,d\theta dx = -2Q$$

This means that with the source distribution $q^{(0)}(x,\theta)$ the sum of the sources inside the fuselage and on its surface vanishes; this is a necessary condition which must be satisfied by $q(x,\theta)$ to ensure that there is no overall flow through the fuselage.

If we write $q(x,\theta)$ in the form

$$q(x,\theta) = q^{(0)}(x,\theta) + \Delta q(x,\theta) \tag{9}$$

then $\Delta q(x,\theta)$ has to satisfy the equation

$$\Delta q(x,\theta) + \frac{1}{2\pi}\int_{0}^{2\pi} \Delta q(x,\theta')d\theta' = -\int_{-\infty}^{\infty}\int_{0}^{2\pi} \frac{[q^{(0)}(x',\theta') - q^{(0)}(x,\theta')][1-\cos(\theta-\theta')]\,d\theta'dx'}{2\pi\sqrt{(x-x')^2 + 2[1-\cos(\theta-\theta')]}^{3}}$$

$$-\int_{-\infty}^{\infty}\int_{0}^{2\pi} \frac{[\Delta q(x',\theta') - \Delta q(x,\theta')][1-\cos(\theta-\theta')]\,d\theta'dx'}{2\pi\sqrt{(x-x')^2 + 2[1-\cos(\theta-\theta')]}^{3}} \qquad \ldots\ldots \tag{10}$$

Precisely as above, when considering a first approximation to equation (4), we may obtain a first approximation to Δq by ignoring the second double integral in equation (10), giving

$$\Delta^{(1)}q(x,\theta) + \Delta^{(1)}\bar{q}(x) = K^{(1)}(x,\theta) \tag{11}$$

where

$$K^{(1)}(x,\theta) = -\int_{-\infty}^{\infty}\int_{0}^{2\pi} \frac{[q^{(0)}(x',\theta') - q^{(0)}(x,\theta')][1-\cos(\theta-\theta')]\,d\theta'dx'}{2\pi\sqrt{(x-x')^2 + 2[1-\cos(\theta-\theta')]}^{3}} . \tag{12}$$

Comparing equation (11) with equation (5), we obtain, similar to equation (8)

$$\Delta^{(1)}q(x,\theta) = K^{(1)}(x,\theta) - \tfrac{1}{2}\bar{K}^{(1)}(x) . \tag{13}$$

Since

$$\int_0^{2\pi} \frac{[1 - \cos(\theta - \theta')]\,d\theta}{\sqrt{(x - x')^2 + 2[1 - \cos(\theta - \theta')]^3}} = k[K(k) - E(k)]$$

where K and E are the complete elliptic integrals (of the first and second kind respectively) with the modulus

$$k^2 = \frac{4}{4 + (x - x')^2} \tag{14}$$

we obtain for the mean value of $K^{(1)}(x,\theta)$

$$\bar{K}^{(1)}(x) = \frac{1}{2\pi} \int_0^{2\pi} K^{(1)}(x,\theta)\,d\theta \tag{15}$$

the relation

$$\bar{K}^{(1)}(x) = -\int_{-\infty}^{\infty} \frac{\bar{q}^{(0)}(x') - \bar{q}^{(0)}(x)}{2\pi} k[K - E]\,dx' \tag{16}$$

with $\bar{q}^{(0)}(x)$ from equation (7).

We have computed values of $\bar{K}^{(1)}(x)$ and of $K^{(1)}(x,\theta)$ for $\theta = 0$, 30°, 60°, 90°. Some values of $\Delta^{(1)}q(x,\theta)$ are plotted in Fig.2 together with values of $q^{(0)}(x,\theta)$. As to be expected, the largest value of $|\Delta^{(1)}q(x,\theta)|$ occurs at $x = 0$, where $\Delta^{(1)}\bar{q}(x = 0) = 0.26\,\bar{q}^{(0)}(x = 0)$.

We note that whilst $\bar{q}^{(0)}(x)$ is everywhere negative, $\Delta^{(1)}\bar{q}(x)$ is positive for $|x| > 0.92$. The integral of the source strength $\Delta^{(1)}q(x,\theta)$ taken over the whole fuselage vanishes:

$$\int_{-\infty}^{\infty} \int_0^{2\pi} \Delta^{(1)}q(x,\theta)\,d\theta dx = 2\pi \int_{-\infty}^{\infty} \Delta^{(1)}\bar{q}(x)\,dx = \pi \int_{-\infty}^{\infty} \bar{K}^{(1)}(x)\,dx = 0 \quad .$$

This follows from

$$\int_{-\infty}^{\infty} \bar{K}^{(1)}(x)dx = -\int_{-\infty}^{\infty} dx \int_{-\infty}^{\infty} \frac{\bar{q}^{(0)}(x') - \bar{q}^{(0)}(x)}{2\pi} \, k[K - E]\, dx'$$

$$= \int_{-\infty}^{\infty} dx' \int_{-\infty}^{\infty} \frac{\bar{q}^{(0)}(x) - \bar{q}^{(0)}(x')}{2\pi} \, k[K - E]\, dx$$

and the fact that k is a function of $(x - x')^2$.

We note also that the difference $|\Delta^{(1)}q(x,\theta) - \Delta^{(1)}\bar{q}(x)|$, i.e. the difference $|K^{(1)}(x,\theta) - \bar{K}^{(1)}(x)|$ is relatively small if we compare it with the difference $|q^{(0)}(x,\theta) - \bar{q}^{(0)}(x)|$. The ratio $\left| \frac{q^{(0)}(x,\theta) - \bar{q}^{(0)}(x)}{\bar{q}^{(0)}(x)} \right|$ varies between $2\sqrt{\frac{x^2}{1 + x^2}}$ and 2. It seems appropriate to measure the difference $|\Delta^{(1)}q(x,\theta) - \Delta^{(1)}\bar{q}(x)|$ in terms of $\bar{q}^{(0)}(x)$. At $x = 0$, the ratio $\left| \frac{\Delta^{(1)}q(x,\theta) - \Delta^{(1)}\bar{q}(x)}{\bar{q}^{(0)}(x)} \right|$ is not larger than 0.032 and for x-values in the range $0 < |x| < 1.5$ it is nowhere larger than 0.05. For $x \simeq 4$, a maximum value of about 0.07 is reached; we have however to note that $\bar{q}^{(0)}(x = 4) = 0.03\, \bar{q}^{(0)}(x = 0)$.

We could determine from equation (10) improved approximations to $\Delta q(x,\theta)$ by the iteration procedure

$$\Delta^{(\nu)}q(x,\theta) + \Delta^{(\nu)}\bar{q}(x) = K^{(1)}(x,\theta)$$

$$- \int_{-\infty}^{\infty} \int_{0}^{2\pi} \frac{[\Delta^{(\nu-1)}q(x',\theta') - \Delta^{(\nu-1)}q(x,\theta')][1 - \cos(\theta - \theta')]\, d\theta' dx'}{2\pi\sqrt{(x - x')^2 + 2[1 - \cos(\theta - \theta')]}^3} \qquad \ldots\ (17)$$

The fact that the difference $|\Delta^{(1)}q(x,\theta) - \Delta^{(1)}\bar{q}(x)|$ is rather small suggests that for $\nu > 1$ the difference between the value of the double integral in equation (17) as a function of θ and its mean value is nearly negligible.

We aim in this Report only towards an accuracy consistent with a small perturbation theory approach. We have therefore computed only mean values of the double integral in equation (17). If we integrate equation (17) with respect to θ, we obtain

$$\Delta^{(\nu)}\bar{q}(x) = \frac{\bar{K}^{(1)}(x)}{2} - \int_{-\infty}^{\infty} \frac{\Delta^{(\nu-1)}\tilde{q}(x') - \Delta^{(\nu-1)}\bar{q}(x)}{4\pi} k[K - E]dx' \quad .$$

With the notation

$$\bar{K}^{(\nu)}(x) = - \int_{-\infty}^{\infty} \frac{\bar{K}^{(\nu-1)}(x') - \bar{K}^{(\nu-1)}(x)}{4\pi} k[K - E]dx'$$

we obtain

$$\Delta^{(\nu)}\bar{q}(x) = \tfrac{1}{2} \sum_{n=1}^{\nu} \bar{K}^{(n)}(x) \quad .$$

Since

$$\int_a^b dx \int_a^b dx' [f(x') - f(x)] F((x - x')^2) = 0$$

we satisfy for each approximation $\Delta^{(\nu)}\bar{q}(x)$ the condition

$$\int_{-\infty}^{\infty} \Delta^{(\nu)}\bar{q}(x)dx = 0 \quad .$$

We have computed values of $\bar{K}^{(n)}(x)$ for $1 \leq n \leq 6$ and found that for every n the largest value of $|\bar{K}^{(n)}(x)|$ occurs at $x = 0$ and that

$$|\bar{K}^{(n)}(x = 0)| < \tfrac{1}{2}|\bar{K}^{(n-1)}(x = 0)| \quad .$$

If the same is true for $n > 6$, then

$$\sum_{n=7}^{\infty} |\bar{K}^{(n)}(x)| < |\bar{K}^{(6)}(x=0)| \sum_{n=1}^{\infty} (\tfrac{1}{2})^n < |\bar{K}^{(6)}(x=0)| \ .$$

With $Q = 1$,

$$2\bar{q}^{(0)}(x=0) = -\frac{1}{\pi} = -0.3183$$

$$\bar{K}^{(1)}(x=0) = -0.0821$$

$$\bar{K}^{(2)}(x=0) = -0.0292$$

$$\bar{K}^{(6)}(x=0) = -0.0009$$

We note that it seems advisable to perform more than the first two steps of the iteration procedure (which give $q^{(1)}(x,\theta) = q^{(0)}(x,\theta) + \Delta^{(1)}q(x,\theta)$), but that we need not go further than $q^{(6)}$.

The approximation to $q(x,\theta)$ used for computing the velocity components induced on the wing and the fuselage reads thus

$$q(x,\theta) = q^{(0)}(x,\theta) + \tfrac{1}{2} \sum_{n=1}^{6} \bar{K}^{(n)}(x) + K^{(1)}(x,\theta) - \bar{K}^{(1)}(x)$$

$$= -2v_{nQ}(x,\theta) + \bar{v}_{nQ}(x) + \tfrac{1}{2} \sum_{n=1}^{6} \bar{K}^{(n)}(x) + K^{(1)}(x,\theta) - \bar{K}^{(1)}(x) \ .$$

... (19)

Some values of $q(x,\theta)$ and of $\bar{q}(x)$ are plotted in Figs.2 and 3. Values of $\sum_{n=1}^{6} \bar{K}^{(n)}(x)$ are tabulated in Table 1.

The function $K^{(1)}(x,\theta)$ has the same properties of symmetry as $v_{nQ}(x,\theta)$, i.e.

$$K^{(1)}(x,\theta) = K^{(1)}(x,\pi-\theta) = K^{(1)}(x,-\theta) = K^{(1)}(-x,\theta) \ .$$

If $K^{(1)}(x,\theta)$ is written as a Fourier series, then only terms of the form $F_n(x) \cos 2n\theta$ arise. Using the numerical values of $K^{(1)}(x,\theta)$ we found that it was sufficient to consider only the first two terms of the Fourier series, i.e. we have used the approximtion:

$$K^{(1)}(x,\theta) - \bar{K}^{(1)}(x) = F_1(x) \cos 2\theta + F_2(x) \cos 4\theta \tag{20}$$

where

$$\left.\begin{aligned} F_1(x) &= \tfrac{1}{3} K^{(1)}(x,0) + \tfrac{1}{3} K^{(1)}(x,30^\circ) - \tfrac{1}{3} K^{(1)}(x,60^\circ) - \tfrac{1}{3} K^{(1)}(x,90^\circ) \\ F_2(x) &= \tfrac{1}{3} K^{(1)}(x,0) - \tfrac{1}{3} K^{(1)}(x,30^\circ) - \tfrac{1}{3} K^{(1)}(x,60^\circ) + \tfrac{1}{3} K^{(1)}(x,90^\circ) \end{aligned}\right\} \tag{21}$$

2.3 Streamwise velocity in the plane through the source line and the axis of the fuselage

We consider now the velocities which the source distribution $q(x,\theta)$ on the fuselage induces in the plane $z = 0$, i.e. the plane through the source line and the axis of the fuselage.

The source distribution produces in $z = 0$ the additional streamwise velocity

$$\begin{aligned} v_{xq}(x,y,0) &= \int_{-\infty}^{\infty} \int_{0}^{2\pi} \frac{q(x',\theta')(x - x')d\theta'dx'}{4\pi\sqrt{(x - x')^2 + (y - \cos\theta')^2 + \sin^2\theta'}^3} \\ &= \int_{-\infty}^{\infty} \int_{0}^{2\pi} \frac{q(x',\theta')(x - x')d\theta'dx'}{4\pi\sqrt{(x - x')^2 + y^2 + 1 - 2y\cos\theta'}^3} \quad . \end{aligned} \tag{22}$$

It produces the spanwise velocity

$$v_{yq}(x,y,0) = \int_{-\infty}^{\infty} \int_{0}^{2\pi} \frac{q(x',\theta')(y - \cos\theta')d\theta'dx'}{4\pi\sqrt{(x - x')^2 + y^2 + 1 - 2y\cos\theta'}^3} \quad . \tag{23}$$

Since the strength of a source element at a point x,θ' is the same as at the point $x,-\theta'$, no velocity component v_z is induced in the plane $z = 0$.

Since

$$q(x,\theta) = q(-x,\theta) \quad ,$$

we have

$$v_{xq}(x,y,0) = - v_{xq}(-x,y,0) \tag{24}$$

and

$$v_{yq}(x,y,0) = v_{yq}(-x,y,0) \quad . \tag{25}$$

Since

$$\int_{-\infty}^{\infty} \frac{(x - x')dx'}{\sqrt{(x - x')^2 + y^2 + 1 - 2y \cos \theta'}^3} = 0$$

and $q(x,\theta) = q(x,-\theta)$, equation (22) can be written in the form

$$v_{xq}(x,y,0) = \int_{-\infty}^{\infty} \int_{0}^{\pi} \frac{[q(x',\theta') - q(x,\theta')](x - x')d\theta'dx'}{2\pi \sqrt{(x - x')^2 + y^2 + 1 - 2y \cos \theta'}^3}$$

$$= \int_{-\infty}^{\infty} \int_{0}^{\pi} \frac{[q(x',\theta') - q(x,\theta') - q(x',\theta = 0) + q(x,\theta = 0)](x - x')d\theta'dx'}{2\pi \sqrt{(x - x')^2 + y^2 + 1 - 2y \cos \theta'}^3}$$

$$+ \int_{-\infty}^{\infty} \frac{(x - x')[q(x',\theta = 0) - q(x,\theta = 0)]dx'}{2\pi} \int_{0}^{\pi} \frac{d\theta'}{\sqrt{(x - x')^2 + y^2 + 1 - 2y \cos \theta'}^3}$$

The integral $\int_{0}^{\pi} \frac{d\theta'}{\sqrt{(x - x')^2 + y^2 + 1 - 2y \cos \theta'}^3}$ can be expressed in terms of the complete elliptic integral E. We introduce the variable τ:

$$\theta' = \pi - 2\tau \quad .$$

With

$$\cos\theta' = -(1 - 2\sin^2\tau)$$

the integral becomes

$$\int_0^{\pi} \frac{d\theta'}{\sqrt{(x-x')^2 + y^2 + 1 - 2y\cos\theta'}^3} = 2\int_0^{\pi/2} \frac{d\tau}{\sqrt{(x-x')^2 + (y+1)^2 - 4y\sin^2\tau}^3}$$

$$= \frac{2}{\sqrt{(x-x')^2 + (y+1)^2}^3} \int_0^{\pi/2} \frac{d\tau}{\sqrt{1 - k^2\sin^2\tau}^3}$$

$$= \frac{2}{\sqrt{(x-x')^2 + (y+1)^2}^3} \frac{E(k)}{1-k^2}$$

$$= \frac{2E(k)}{[(x-x')^2 + (y-1)^2]\sqrt{(x-x')^2 + (y+1)^2}} \quad \ldots\ (26)$$

with

$$k^2 = \frac{4y}{(x-x')^2 + (y+1)^2} \quad (27)$$

$v_{xq}(x,y,0)$ can thus be evaluated from the equation:

$$v_{xq}(x,y,0) = \int_{-\infty}^{\infty}\int_0^{\pi} \frac{[q(x',\theta') - q(x,\theta') - q(x',\theta=0) + q(x,\theta=0)](x-x')d\theta'dx'}{2\pi\sqrt{(x-x')^2 + y^2 + 1 - 2y\cos\theta'}^3}$$

$$+ \int_{-\infty}^{\infty} \frac{[q(x',\theta=0) - q(x,\theta=0)](x-x')E(k)\,dx'}{\pi[(x-x')^2 + (y-1)^2]\sqrt{(x-x')^2 + (y+1)^2}} \quad (28)$$

with k given by equation (27).

The numerical evaluation of the double integral does not cause any difficulty, except for $y = 1$, $x \to 0$, since the integrand is free from singularities.

For $y > 1$, the denominator of the double integral nowhere vanishes. Since $q(x,\theta) = q(-x,\theta)$, the integral is zero for $x \to 0$. The same is not true for $y \to 1$; in Appendix A it is shown that for $x \to 0$ the double integral does not vanish and that

$$\lim_{x\to 0} v_x(x > 0,\ y = 1,\ z = 0) = -0.05305$$

When evaluating the single integral for $y = 1$, we find that as $x' \to x$ the limiting value of the integrand is $\frac{-1}{2\pi}\frac{\partial q(x,\theta=0)}{\partial x}$. For $y = 1$, $x \to 0$ the single integral tends to zero.

We intend to extend the present work for an unswept infinite source line to swept source lines and later to swept wings of finite span. We are therefore interested to know how important the term $K^{(1)}(x,\theta) - \bar{K}^{(1)}(x)$ of the source distribution $q(x,\theta)$ is with respect to the induced v_x velocity, because the amount of computation is considerably reduced if we have to evaluate only the single integrals $\bar{K}^{(n)}(x)$ and not the double integral $K^{(1)}(x,\theta)$.

We have therefore computed

$$\Delta v_x^*(x,y,0) = \int_{-\infty}^{\infty}\int_{0}^{\pi} \frac{[\Delta^* q(x',\theta') - \Delta^* q(x,\theta')](x - x')d\theta' dx'}{2\pi\sqrt{(x - x')^2 + y^2 + 1 - 2y\cos\theta'}^3} \qquad (29)$$

for

$$\Delta^* q(x,\theta) = K^{(1)}(x,\theta) - \bar{K}^{(1)}(x) = F_1(x)\cos 2\theta + F_2(x)\cos 4\theta\ . \qquad (30)$$

The integrals $\int_0^{\pi} \frac{\cos 2n\theta'}{\sqrt{(x - x')^2 + y^2 + 1 - 2y\cos\theta'}^3}\, d\theta'$ can be expressed in terms of complete elliptic integrals.

$$\Delta v_x^*(x,y,0) =$$

$$= \frac{1}{8\pi y^{3/2}} \int_{-\infty}^{\infty} \left\{ [F_1(x') - F_1(x)] \left[\left(\frac{k^3}{1-k^2} + \frac{16}{k} \right) E - \frac{8(2-k^2)}{k} K \right] \right.$$

$$+ [F_2(x') - F_2(x)] \left[\frac{k^3}{1-k^2} E + \frac{128}{k^5} \left(\frac{16}{5} - \frac{16}{5} k^2 + \frac{7}{10} k^4 \right) E \right.$$

$$\left. \left. - \frac{32(2-k^2)}{k} K + \frac{128}{k^5} \left(-\frac{16}{5} + \frac{24}{5} k^2 - \frac{8}{5} k^4 \right) K \right] \right\} (x - x') dx' \quad \ldots\ (31)$$

where k is given by equation (27). As x tends to zero, $\Delta v_x^*(x,y,0)$ tends to zero for all valus $y \geq 1$.

Δv_x^* has for $y = R$ the largest value, 0.0015, at $x/R = 0.15$ and the smallest value, -0.0009, at $x/R = 1$. These values of $|\Delta v_x^*|$ are sufficiently small that they may be neglected in future computations.

Calculated values of the streamwise velocity induced by the source distribution $q(x,\theta)$ on the fuselage, v_{xq}, are given in Table 2 and are plotted in Fig.4.

The source line itself induces in the wing plane, $z = 0$, the streamwise velocity $\frac{v_{xQ}}{Q/R} = \frac{1}{2\pi\, x/R}$; we have added in Fig.4 the curve $-0.2 v_{xQ}$.

We learn from Fig.4 that the interference velocity is of opposite sign to the velocity of the source line itself, as is to be expected since the mean value of the source strength, $\bar{q}(x)$, is everywhere negative. We learn further that the source distribution on the fuselage induces a much smaller velocity than the source line itself.

This result differs from that for the downwash of a straight vortex line crossing a circular cylindrical fuselage. $v_{z\Gamma}$ and v_{zq} (= Δv_z of Fig.3 in Ref.1) have the same sign. At $x/R = 1$, $y/R = 1$ the downwash due to the body interference is about half that due to the isolated vortex and at $x/R = 5$, $y/R = 1$ the two are nearly equal. This different behaviour of the interference velocities for large $|x|$ is due to the fact that the modulus of the

normal velocity induced by the vortex line $\left(v_{n\Gamma} = \frac{\Gamma}{2\pi} \frac{-x \sin\theta}{x^2 + \sin^2\theta}\right)$ decreases for $|x| > 1$ less with increasing $|x|$ than the normal velocity induced by the source line $\left(v_{nQ} = \frac{Q}{2\pi} \frac{\sin^2\theta}{x^2 + \sin^2\theta}\right)$.

In Ref.4, it has been suggested that the body effect on the displacement flow past a wing might be estimated by means of a source distribution along the axis of the fuselage. The strength of the axial source distribution, $E(x)$, at a station x was taken as equal to the spanwise integral of that part of the source distribution of the gross wing which is inside the fuselage, with opposite sign. This means that for an isolated unswept source line a single sink of strength 2RQ would be taken.

To judge how good an approximation is achieved by a single sink we compare in Fig.5 the streamwise velocity in the wing-body junction produced by the single sink situated at $x = y = z = 0$ $\left(\frac{Q}{2\pi} \frac{x}{\sqrt{x^2 + 1}^3}\right)$ with the velocity $v_{xq}(x,1,0)$ produced by the source distribution $q(x,\theta)$. The single sink produces, of course, no streamwise velocity at $x = 0$. The source distribution produces a velocity which varies discontinuously at $x = 0$; the mean value at $x = 0$ vanishes also. Fig.5 shows that for $|x/R| > 0.3$ the single sink produces too large a value of $-v_x$. This explains the statement in Ref.4 that the 'source method' tends to overestimate the interference effect in the junction.

We may further note that the streamwise velocity induced in the wing plane by the single sink situated at $x = y = z = 0$ decreases for $x/R > 0.5$ more rapidly with increasing spanwise distance y than the velocity $-v_{xq}(x,y,0)$ induced by the source distribution on the fuselage.

We have also plotted in Fig.5 the streamwise velocities which are induced by the mean source distributions $\bar{q}(x)$ and $\bar{q}^{(0)}(x)$ on the fuselage, i.e. source distributions which do not vary with θ. These are calculated from the relation

$$v_{xq}(x,y,0) = \frac{1}{\pi} \int_{-\infty}^{\infty} \frac{[\bar{q}(x') - \bar{q}(x)](x - x')\,E\,dx'}{\sqrt{(x - x')^2 + (y + 1)^2}\,[(x - x')^2 + (y - 1)^2]} \qquad (32)$$

with k given by equation (27). These source distributions produce, of course, a velocity which varies continuously and therefore vanishes at $x = 0$.

Finally, we have plotted the velocity produced by the first approximation to the source distribution on the fuselage, $q^{(0)}(x,\theta)$. The difference between the velocities for $q(x,\theta)$ and $q^{(0)}(x,\theta)$ is the sum of the difference between the velocities related to $\bar{q}(x)$ and $\bar{q}^{(0)}(x)$ and the term Δv_x^* of equation (31).

2.4 Streamwise velocity on the fuselage

The isolated infinitely long fuselage does not produce any perturbation to the flow field. Thus the pressure distribution on the fuselage is entirely due to the presence of the wing.

We determine in this section the velocity due to a single source line in the presence of the fuselage. The isolated source line produces the streamwise velocity

$$v_{xQ}(x,\theta) = \frac{Q}{2\pi} \frac{x}{x^2 + \sin^2\theta} . \tag{33}$$

The source distribution $q(x,\theta)$ produces the additional streamwise velocity

$$v_{xq}(x,\theta) = \int_{-\infty}^{\infty} \int_{0}^{2\pi} \frac{q(x',\theta')\,(x - x')\,d\theta' dx'}{4\pi\sqrt{(x - x')^2 + 2[1 - \cos(\theta - \theta')]}^3} \tag{34}$$

Now

$$\int_0^{2\pi} \frac{d\theta'}{\sqrt{(x - x')^2 + 2[1 - \cos(\theta - \theta')]}^3} = \frac{4\,E(k)}{(x - x')^2\sqrt{(x - x')^2 + 4}} \tag{35}$$

with

$$k^2 = \frac{4}{4 + (x - x')^2} \tag{36}$$

Therefore

$$v_{xq}(x,\theta) = \int_{-\infty}^{\infty}\int_{0}^{2\pi} \frac{[q(x',\theta') - q(x,\theta')](x - x')d\theta'dx'}{4\pi\sqrt{(x - x')^2 + 2[1 - \cos(\theta - \theta')]}^3}$$

$$= \int_{-\infty}^{\infty}\int_{0}^{2\pi} \frac{[q(x',\theta') - q(x,\theta') - q(x',\theta) + q(x,\theta)](x - x')d\theta'dx'}{4\pi\sqrt{(x - x')^2 + 2[1 - \cos(\theta - \theta')]}^3}$$

$$+ \int_{-\infty}^{\infty} \frac{[q(x',\theta) - q(x,\theta)]\,E(k)}{\pi(x - x')\sqrt{(x - x')^2 + 4}}\,dx' \qquad (37)$$

with k from equation (36).

The numerical evaluation of $v_{xq}(x,\theta)$ does not cause any difficulty for $x \neq 0$. $v_{xq}(x,\theta)$ is for $\theta \neq 0$ a continuous antisymmetric function with respect to x and therefore $v_{xq}(x = 0, \theta \neq 0) = 0$. For $\theta \equiv 0$ we have already determined the limit $v_{xq}(x \to 0, \theta = 0)$ since for $\theta = 0$ the v_{xq} from equation (37) is of course the same as $v_{xq}(x, y = 1, z = 0)$ from equation (28).

Calculated values of $v_{xq}(x,\theta)$ are given in Table 3 and are plotted in Fig.6. These suggest that the limit of $v_{xq}(x,\theta)$ as x and θ tend to zero depends on the manner in which θ tends to zero, i.e. if $\theta = \kappa x$ and $x \to 0$ the limit of $v_{xq}(x,\theta)$ differs from the limit obtained for $\theta \equiv 0$.

The single integral in equation (37) vanishes for $\theta = 0$ and $x \to 0$, but has a non-zero value for $\theta = \kappa x$ and $x \to 0$. It is shown in Appendix C that the limit of the single integral as x tends to zero has the minimum value $-\frac{1}{4\pi}$ when $\theta = x$.

In Fig.7, we have plotted for the top of the fuselage, $\theta = 90^{\circ}$, the streamwise velocity induced by the source line v_{xQ}, the velocity induced by the source distribution on the fuselage, v_{xq}, and the total interference velocity $v_x = v_{xQ} + v_{xq}$. We have also plotted the velocity induced by a single sink of strength $2Q$ situated at $x = y = z = 0$ and note that this gives a good approximation to $v_{xq}(x, \theta = 90^{\circ})$.

We may mention that the contribution to $v_{xq}(x,\theta)$ produced by $\Delta^* q(x,\theta)$ of equation (30) is of little importance everywhere on the fuselage, the largest and the smallest values of Δv^*_{xq} are 0.0015 and -0.0011 respectively.

2.5 Circumferential velocity on the fuselage

Finally, we consider the circumferential velocity, v_θ, on the fuselage. The isolated source line produces the velocity

$$v_{\theta Q} = -v_y \sin\theta + v_z \cos\theta$$

$$= \frac{Q}{2\pi} \frac{\sin\theta \cos\theta}{x^2 + \sin^2\theta} \quad . \tag{38}$$

The source distribution $q(x,\theta)$ produces the additional velocity

$$v_{\theta q}(x,\theta) =$$

$$= \int_{-\infty}^{\infty} \int_{0}^{2\pi} \frac{q(x',\theta')[-(\cos\theta - \cos\theta')\sin\theta + (\sin\theta - \sin\theta')\cos\theta]\,d\theta'dx'}{4\pi\sqrt{(x-x')^2 + 2[1-\cos(\theta-\theta')]}^3}$$

$$= \int_{-\infty}^{\infty} \int_{0}^{2\pi} \frac{q(x',\theta')\sin(\theta-\theta')\,d\theta'dx'}{4\pi\sqrt{(x-x')^2 + 2[1-\cos(\theta-\theta')]}^3}$$

$$= \int_{-\infty}^{\infty} \int_{0}^{2\pi} \frac{[q(x',\theta') - q(x,\theta')]\sin(\theta-\theta')\,d\theta'dx'}{4\pi\sqrt{(x-x')^2 + 2[1-\cos(\theta-\theta')]}^3}$$

$$+ \int_{0}^{2\pi} \frac{q(x,\theta')\sin(\theta-\theta')\,d\theta'}{4\pi[1-\cos(\theta-\theta')]} \tag{39}$$

$$v_{\theta q}(x,\theta) = \int_{-\infty}^{\infty} \int_{0}^{2\pi} \frac{[q(x',\theta') - q(x,\theta') - q(x',\theta)+q(x,\theta)] \sin(\theta - \theta')d\theta'dx'}{4\pi\sqrt{(x - x')^2 + 2[1 - \cos(\theta - \theta')]}^3}$$

$$+ \int_{0}^{2\pi} \frac{[q(x,\theta') - q(x,\theta)][1 + \cos(\theta - \theta')]d\theta'}{4\pi \sin(\theta - \theta')} \quad . \qquad (40)$$

The numerical evaluation of $v_{\theta q}$ from equation (40) is straightforward except for the case $x = 0$, $\theta \to 0$. Due to the properties of symmetry of $q(x,\theta)$, the circumferential velocity vanishes for $\theta = 90^{o}$ and for $\theta = 0$ except for $x = 0$. It is shown in Appendix A that

$\lim_{\theta \to 0} v_{\theta q}(x = 0,\theta) = - \lim_{x \to 0} v_{xq}(x > 0, y = 1, z = 0) = 0.05305$. The limiting value of $v_{\theta q}$ as x and θ tend to zero simultaneously depends again on the manner in which x and θ tend to zero. If $x = \kappa\theta$ and $\theta \to 0$, then the single integral in equation (40) has the same behaviour as the single integral in equation (37); it reaches a maximum value of $\frac{1}{4\pi}$ when $\kappa = 1$.

Calculated values of $v_{\theta q}$ are given in Table 4 and are plotted in Fig.8. For small values of x the ratio between $v_{\theta q}(x,\theta)$ and $v_{\theta 0}(x,\theta)$ is not larger than about 0.2, the ratio increases to about 0.7 for $x = 1$ and increases to slightly more than 1 for $x = 3$.

When evaluating $v_{\theta q}(x,\theta)$ from equation (40), we have used for the source strength $q(x,\theta)$ the approximation

$$q(x,\theta) = q^{(0)}(x,\theta) + \tfrac{1}{2} \sum_{n=1}^{6} \bar{K}^{(n)}(x) \quad .$$

Equation (40) implies that the terms $\bar{v}_n(x)$ and $\Sigma\bar{K}^{(n)}(x)$ do not contribute to the value of $v_{\theta q}$. We have ignored the term $\Delta^*q(x,\theta) = K^{(1)}(x,\theta) - \bar{K}^{(1)}(x)$ in equation (19); the contribution of $\Delta^*q(x,\theta)$ is small because $F_1(x)$ and $F_2(x)$ in equation (30) are small. Thus to a high degree of accuracy the circumferential components $v_{\theta q}$ can be considered to come only from the first approximation $q^{(0)}(x,\theta)$.

3 PRESSURE DISTRIBUTIONS ON WING-FUSELAGE COMBINATIONS

3.1 Pressure distribution on the wing according to first-order theory

The calculated velocity components due to an isolated source line in the presence of the fuselage can be used to determine the pressure distribution on a straight wing of given section shape when attached to a fuselage in midwing position.

Within first-order theory, the strength of the source distribution $q_w(x,y)$ which represents the isolated wing in a mainstream of velocity V_0 parallel to the wing chord is such that the normal velocity in the wing plane $v_z(x,y,z = 0)$ satisfies the boundary condition to first order, i.e.

$$v_z(x,y,z = 0) = V_0 \frac{\partial z_t(x,y)}{\partial x} \tag{41}$$

where $z = z_t(x,y)$ gives the shape of the wing. In the following, we make all velocity components dimensionless with V_0 and take $V_0 = 1$.

We have noted that the source distribution $q(x,\theta)$ on the fuselage does not induce a velocity component $v_z(x,y,z = 0)$ in the plane $z = 0$; therefore, the source distribution in the wing plane $q_w(x,y)$ is the same for the wing-fuselage combination as for the isolated wing.

A planar source distribution $q_w(x,y)$ induces in $z = 0$ the normal velocity

$$v_z(x,y,z = 0) = \tfrac{1}{2} q_w(x,y) \quad . \tag{42}$$

We consider in this Report only wings of constant chord and constant section shape along the span, so that

$$q_w(x,y) = 2 \frac{dz_t(x)}{dx} \quad . \tag{43}$$

To determine the change in the pressure distribution due to the fuselage - to first-order accuracy - we have to determine only the change in the streamwise velocity

$$\Delta v_x(x,y,z=0) = \int_0^{c/R} q_w(x') \frac{v_{xq}\left(\frac{x}{R} - \frac{x'}{R}, \frac{y}{R}, 0\right)}{Q/R} d\left(\frac{x'}{R}\right) \tag{44}$$

and by equation (43)

$$\Delta v_x(x,y,0) = 2\frac{c}{R} \int_0^1 \frac{dz_t/c}{dx'/c} \frac{v_{xq}\left(\frac{x}{R} - \frac{x'}{R}, \frac{y}{R}, 0\right)}{Q/R} d\left(\frac{x'}{c}\right) \tag{45}$$

where c is the wing chord and the values of $\frac{v_{xq}}{Q/R}$ can be taken from Table 2.

For the 10 per cent thick RAE 101 section we have computed $\Delta v_x(x,y = R,0)$ for various values of the ratio c/R and plotted the results in Fig.9. To assist in assessing the importance of the interference effect, we have plotted also $-0.1v_{xw}(x)$, where v_{xw} is the streamwise velocity perturbation of the isolated wing.

Fig.9 shows that, except close to the leading edge and near the trailing edge, the velocity is reduced (a fact which is well-known from experiment). Δv_x vanishes when c/R tends to zero, since $c/R \to 0$ represents the case of a straight wing attached to an infinite reflection plate parallel to the main stream, which for inviscid flow does not alter the flow. Δv_x vanishes also when c/R tends to infinity, i.e. when, for a wing of given size, the body disappears (Δv_x behaves for large c/R as $\frac{1}{c/R} \log \frac{c}{R}$). We note that according to the first-order theory the interference velocity is not larger than 20% of the perturbation velocity of the isolated wing. This result is to be expected from the comparison in Fig.4 between v_{xq} and v_{xQ}, where we note that the magnitude of the interference velocity, $-v_{xq}(x,y = R,0)$, is nowhere larger than one fifth of the velocity from the isolated source line. The maximum reduction in velocity occurs in the neighbourhood of the position of the maximum thickness of the wing. This is to be expected from a consideration of a planview of some streamlines on the wing, as sketched e.g. in Fig.X.4 of Ref.5. If one makes the assumption that one streamline follows the junction line

between wing and body, then this latter streamline departs furthest from the straight line $y = R$ at the position of the maximum thickness. One can therefore assume that the distance between neighbouring streamlines is largest at this chordwise position. The values of Δv_x close to the leading edge are unreliable due to the shortcomings of the source distribution $q_w^{(1)}(x)$ close to the leading edge.

As a further example, we have plotted in Fig.10 the velocity decrement in the junction at the maximum thickness position for a wing of biconvex parabolic arc section. The figure shows a similar variation of Δv_x as function of c/R and similar values of $\Delta v_x / v_{xw}$ as shown in Fig.9 for the RAE 101 section.

We have mentioned in section 2.3 the suggestion of Ref.4 to estimate the interference effect by means of a sink distribution on the axis, which is equivalent to the approximation

$$- \frac{v^*_{xq}(x, y = R)}{c/R} = \frac{1}{2\pi} \frac{x/R}{\sqrt{1 + (x/R)^2}^3} \qquad (46)$$

see also Fig.5. With the parabolic arc section $z_t = 2t \frac{x}{c}\left(1 - \frac{x}{c}\right)$, this gives for $x/c = 0.5$

$$- \frac{\Delta^* v_x (x/c = 0.5, y = R)}{t/c} = \frac{4}{\pi} \left[\frac{2}{c/R} \log \left(0.5 \frac{c}{R} + \sqrt{1 + 0.25 \left(\frac{c}{R}\right)^2} \right) - \frac{1}{\sqrt{1 + 0.25 \left(\frac{c}{R}\right)^2}} \right]$$

... (47)

We have plotted $\Delta^* v_x$ in Fig.10. The figure shows - as expected from Fig.5 - that, for $c/R > 1$, $\Delta^* v_x$ overestimates the interference velocity Δv_x noticeably.

For the RAE 101 section and $c/R = 5$, we have also calculated the velocity decrement at some spanwise stations away from the junction. The results are plotted in Fig.11. We note that the maximum value of the interference velocity varies approximately linearly with the inverse of the spanwise distance, i.e. as $\frac{1}{y/R}$. We may remind ourselves that the interference downwash induced by a

lifting wing in the presence of the fuselage varies nearly as $\frac{1}{(y/R)^2}$, see Figs.4 and 8 of Ref.1.

3.2 Pressure distribution on the wing according to second-order theory

It is of some interest to know the interference velocities somewhat more accurately than the results from first-order theory. To obtain the pressure coefficient to a higher accuracy, one has first to satisfy the boundary condition to more than first-order accuracy, secondly one has to take account of the fact that the velocity at the surface of the wing differs somewhat from the velocity induced in the plane $z = 0$, and finally when computing the pressure coefficient, one has to take account of all velocity components instead of using the first order approximation, $c_p^{(1)} = -2v_x^{(1)}$.

Let us first consider the boundary condition. At the surface of the wing, $z = z_t(x,y)$, the velocity field has to satisfy the equation

$$[V_o + v_x(x,y,z_t)]\frac{\partial z_t}{\partial x} + v_y(x,y,z_t)\frac{\partial z_t}{\partial y} - v_z(x,y,z_t) = 0 \quad . \tag{48}$$

With the present case of an unswept wing of constant section shape $\partial z_t/\partial y = 0$ so that the boundary condition on the wing reads

$$[1 + v_x(x,y,z_t)]\frac{\partial z_t}{\partial x} = v_z(x,y,z_t) \quad . \tag{49}$$

We intend to retain in this equation all terms of order $(t/c)^2$. The left hand side can be approximated, correct to second order, by

$$[1 + v_{xw}^{(1)}(x,z = 0) + \Delta v_x^{(1)}(x,y,0)]\frac{dz_t}{dx}$$

where $v_{xw}^{(1)}$ and $\Delta v_x^{(1)}$ are computed from the first-order source distribution

$$q_w^{(1)}(x) = 2\frac{dz_t}{dx} \quad .$$

We intend to satisfy the boundary condition again by a source distribution in the plane of the wing and a source distribution on the fuselage. (Such a configuration of singularities would not permit us to satisfy the exact boundary condition, to do this a singularity distribution at the surface of the wing would be required.) The source distribution in the wing plane is expressed

as the sum of two terms $q_w^{(2)}(x) + \Delta q(x,y)$, where $q_w^{(2)}(x)$ is the source distribution of the isolated gross wing, correct to second order, and $\Delta q(x,y)$ is an interference term. The source distribution on the fuselage, $q_f(x,\theta)$, is related to $q_w^{(2)}(x)$:

$$q_f(x,\theta) = \int_0^{c/R} q_w^{(2)}\left(\frac{x'}{R}\frac{R}{c}\right) q\left(\frac{x}{R} - \frac{x'}{R}, \theta\right) d\left(\frac{x'}{R}\right) \qquad (50)$$

with $q\left(\frac{x}{R} - \frac{x'}{R}, \theta\right)$ from equation (19), i.e. the two distributions $q_w^{(2)}(x)$ and $q_f(x,\theta)$, taken together, satisfy the boundary condition on the fuselage.

The interference term $\Delta q(x,y)$ varies along the span, therefore we cannot yet determine without much computation the related $\Delta q_f(x,\theta)$ which would make the fuselage a stream surface. Therefore we do not take full account of the interference between $\Delta q(x,y)$ and the fuselage but determine the effect of $\Delta q(x,y)$ as if this source distribution were acting in the presence of an infinite reflection plate, situated in the wing-body junction.

Let us now consider the contributions to the velocity component $v_z(x,y,z_t)$ induced by the various source distributions. We approximate the contribution $v_z^{(1)}(x,y,z_t)$ induced by $q_w^{(1)}(x)$ by the first two terms in the Taylor's series expansion

$$v_z^{(1)}(x,y,z_t) = v_z^{(1)}(x,y,0) + z_t \left(\frac{\partial v_z^{(1)}(x,y,z)}{\partial z}\right)_{z=0}$$

$$= \frac{q_w^{(1)}(x)}{2} - z_t \frac{dv_{xw}^{(1)}(x, z=0)}{dx} \qquad (51)$$

The strengths of the source distributions $q_w^{(2)}(x) - q_w^{(1)}(x)$ and $\Delta q(x,y)$ are both of second order, we can therefore approximate their contributions to $v_z(x,y,z_t)$ by the v_z in the plane $z = 0$, i.e. by

$$\frac{q_w^{(2)}(x) - q_w^{(1)}(x)}{2} + \frac{\Delta q(x,y)}{2} .$$

The velocity $\Delta v_z(x,y,z_t)$ induced by the source distribution on the fuselage, $q_f(x,\theta)$, has to be evaluated numerically, since we do not know the derivative $\left(\frac{\partial \Delta v_z}{\partial z}\right)_{z=0}$. We know that

$$\left(\frac{\partial \Delta v_z}{\partial z}\right)_{z=0} = -\frac{\partial \Delta v_x(x,y,0)}{\partial x} - \frac{\partial \Delta v_y(x,y,0)}{\partial y} \tag{52}$$

but we have not computed $\Delta v_y(x,y,0)$, except in the wing-body junction where $\Delta v_y(x,y = R,\ z = 0) = 0$.

We shall compute the velocity in the wing-body junction, Δv_{zJ}.

The velocity component v_z on the surface of the fuselage can be determined from the circumferential and the normal velocity components

$$v_z(x,\theta) = \cos\theta\, v_\theta(x,\theta) + \sin\theta\, v_n(x,\theta) \tag{53}$$

For the source distribution $q(x,\theta)$ on the fuselage given by

$$q(x,\theta) = q^{(0)}(x,\theta) + \tfrac{1}{2}\sum_{n=1}^{6} \bar{K}^{(n)}(x)$$

we have determined the circumferential velocity component $v_{\theta q}$ in section 2.5 and calculated values have been tabulated in Table 4. The normal velocity component v_{nq} is known since it is equal to the negative value of v_{nQ}, given by equation (1). Values of v_{zq} are plotted in Fig.12. We note from Figs.8 and 12 that, for small θ and x, the values of $v_{\theta q}$ and v_{zq} are noticeably different, because v_{nq} is, for small x and θ, a rapidly varying function of x and θ.

With $v_{zq}(x,\theta)$, the velocity in the wing-body junction, $z_t(x) = R \sin\theta_J(x)$, can be calculated from

$$\Delta v_{zJ}(x,\theta_J(x)) = \frac{c}{R}\int_0^1 q_w(x') \frac{v_{zq}\left(\left(\frac{x}{c} - \frac{x'}{c}\right)\frac{c}{R};\ \theta_J\right)}{Q/R}\, d\left(\frac{x'}{c}\right). \tag{54}$$

Using for $q_w(x)$ the approximation from first-order theory, equation (43), we have computed the Δv_{zJ} for two wing-body configurations derived from a wing with a 10 per cent thick RAE 101 section. The results are plotted in Fig.13, together with a multiple of the v_{zw} of the wing alone according to first-order theory, $v^{(1)}_{zw} = dz_t/dx$. The figure shows that the interference Δv_{zJ} is of the order of 10 per cent of the basic $v^{(1)}_{zw}$. The factor of c/R on the right-hand side of equation (54) explains why $|\Delta v_{zJ}|$ in Fig.13 is so much larger for $c/R = 5$ than for $c/R = 2$. For given t/c, the ratio t/R and with it $\theta_J(x)$ increase also with increasing c/R, but we see from Fig.12 that the variation of $v_{zq}(x,\theta)$ with θ, i.e. whether it increases or decreases with increasing θ, depends on the values of x and θ.

Since $\Delta v_z(x,y,0) = 0$ we obtain from the Taylor's series expansion and from equation (52) the approximation:

$$\Delta v_{zJ} \simeq - z_t \left[\frac{\partial \Delta v_x(x,y = R,0)}{\partial x} + \frac{\partial \Delta v_y(x,y = R,0)}{\partial y} \right] . \qquad (55)$$

We have computed $\Delta v_x(x,y = R,0)$, see Figs.9 and 11, and can thus evaluate the term $- z_t \frac{\partial \Delta v_x}{\partial x}$ of equation (55). We find that for most x-values $\left| z_t \frac{\partial \Delta v_x}{\partial x} \right|$ is noticeably smaller than $|\Delta v_{zJ}|$; it is about $0.15|\Delta v_{zJ}|$. This implies that $|\partial \Delta v_y/\partial y|$ is not negligibly small in the junction, but we may expect that it decreases rapidly with increasing y. This implies that we may expect that $|\Delta v_{zJ}|$ decreases rapidly.

We have not yet computed $v_{zq}(x,y,z)$ induced by the source distribution on the fuselage for points away from the fuselage $y^2 + z^2 > R^2$, $z > 0$. This would require the evaluation of

$$v_{zq}(x,y,z) = \int_{-\infty}^{\infty} \int_{0}^{2\pi} \frac{q(x',\theta')(z - \sin\theta')d\theta'dx'}{4\pi\sqrt{(x - x')^2 + (y - \cos\theta')^2 + (z - \sin\theta')^2}^3} . \qquad (56)$$

To estimate the effect of $\Delta v_z(x,y,z = z_t)$ we can therefore only make a crude assumption. We choose

$$\Delta v_z(x,y,z_t) = \Delta v_{zJ}(x)\left(2 - \left|\frac{y}{R}\right|\right)^2 \qquad \text{for } 1 < \left|\frac{y}{R}\right| < 2$$

$$= 0 \qquad \text{for } \left|\frac{y}{R}\right| > 2 \,. \tag{57}$$

Inserting the various contributions to the velocity components into equation (49) we obtain the equation

$$\left[1 + v_{xw}^{(1)}(x,z=0) + \Delta v_x^{(1)}(x,y,0)\right]\frac{dz_t}{dx} = \frac{q_w^{(1)}(x)}{2} - z_t\frac{dv_{xw}^{(1)}(x,z=0)}{dx} + \frac{q_w^{(2)}(x) - q_w^{(1)}(x)}{2} + \frac{\Delta q(x,y)}{2} + \Delta v_z(x,y,z_t) \tag{58}$$

The boundary condition for the isolated wing, which reads

$$\left[1 + v_{xw}^{(1)}(x,0)\right]\frac{dz_t}{dx} = q_w^{(2)}(x) - z_t\frac{dv_{xw}^{(1)}(x,0)}{dx}$$

gives for the source distribution $q_w^{(2)}(x)$ the equation

$$q_w^{(2)}(x) = 2\left[\frac{dz_t}{dx} + \frac{d}{dx}\left(z_t v_{xw}^{(1)}\right)\right] \tag{59}$$

When we insert this relation into equation (58), then we obtain for the interference term of the source distribution in the wing plane the equation

$$\Delta q(x,y) = 2\Delta v_x^{(1)}(x,y,0)\frac{dz_t}{dx} - 2\Delta v_z(x,y,z_t) \tag{60}$$

We shall now examine in turn the relative magnitude of the effects produced by the two terms in equation (60):

With the assumed spanwise variation of Δv_z given by equation (57), we obtain for the streamwise velocity component in the wing-body junction induced by the source distribution $\Delta^* q(x,y) = -2\Delta v_z(x,y,z)$ the equation

$$- \Delta^* v_{xJ}(x) = \int_0^c \frac{v_{zJ}(x')}{\pi} \int_0^R \left(1 - \frac{y'}{R}\right)^2 \frac{(x - x')dy'dx'}{\sqrt{(x - x')^2 + y'^2}^3}$$

$$= \int_0^{c/R} \frac{v_{zJ}\left(\frac{x'}{R}\right)}{\pi} \left(\frac{x}{R} - \frac{x'}{R}\right) \left[\frac{\sqrt{\left(\frac{x - x'}{R}\right)^2 + 1}}{\left(\frac{x}{R} - \frac{x'}{R}\right)^2} - \frac{2}{\left|\frac{x - x'}{R}\right|} \right.$$

$$\left. + \log \frac{1 + \sqrt{\left(\frac{x - x'}{R}\right)^2 + 1}}{\left|\frac{x - x'}{R}\right|} \right] d\left(\frac{x'}{R}\right) . \qquad (61)$$

Values of $- \Delta v^*_{xJ}$ have been computed for the two distributions of Δv_{zJ} plotted in Fig.13; the results are shown in Fig.14. If we compare Fig.14 with Figs.9 and 11 then we note that $\Delta q(x,y)$ has increased the velocity decrement at the maximum thickness position caused by the body interference by 30% for $c/R = 2$ and by 25% for $c/R = 5$.

If we assume that $\Delta v_x^{(1)}(x,y,0)$ varies along the span as $\frac{1}{y/R}$, as suggested by Fig.11, then the source distribution $\Delta q^{**}(x,y) = 2\Delta v_x^{(1)}(x,y,0) \frac{dz_t}{dx}$ induces in the wing-body junction the velocity

$$\Delta^{**} v_{xJ}(x) = \int_0^c \frac{\Delta v_{xJ}^{(1)}(x')}{\pi} \frac{dz_t}{dx'} \int_R^\infty \frac{1}{y'/R} \frac{(x - x')dx'dy'}{\sqrt{(x - x')^2 + (y' - R)^2}^3}$$

$$= \int_0^{c/R} \frac{\Delta v_{xJ}\left(\frac{x'}{R}\right)}{\pi} \frac{dz_t}{dx'} \left\{ \frac{1 - \left|\frac{x - x'}{R}\right|}{\frac{x - x'}{R}\left[1 + \left(\frac{x - x'}{R}\right)^2\right]} - \frac{\frac{x-x'}{R}}{\sqrt{1 + \left(\frac{x - x'}{R}\right)^2}^3} \times \right.$$

$$\left. \log \frac{\sqrt{1 + \left(\frac{x-x'}{R}\right)^2} - 1}{\left(\frac{x-x'}{R}\right)^2 + \sqrt{\left(\frac{x-x'}{R}\right)^2\left[1 + \left(\frac{x-x'}{R}\right)^2\right]}} \right\} d\left(\frac{x'}{R}\right) . \qquad (62)$$

For the 10 per cent thick RAE 101 section and $c/R = 5$, equation (62) gives at the maximum thickness position the value $-\Delta^{**}v_{xJ} = 0.001$. We shall therefore ignore the term $\Delta^{**}v_{xJ}$.

The velocity decrement in the junction at the maximum thickness position is somewhat further increased when we compute $\Delta v_x(x,y = R,0)$ by equation (44) with $q_w^{(2)}(x)$ instead of $q_w^{(1)}(x)$. The effect of the difference $q_w^{(2)}(x) - q_w^{(1)}(x)$ on $\Delta v_x(x,y = R, z = 0)$ is shown in Fig.15.

Up to now, we have considered the streamwise velocity only in the plane $z = 0$. We want now to study the velocity at the surface of the wing. We obtain the perturbation velocity correct to second order from the Taylor's series expansion

$$v_x(x,y,z_t) = v_x(x,y,0) + z_t \left(\frac{\partial v_x(x,y,z)}{\partial z} \right)_{z=0}$$

$$= v_x(x,y,0) + z_t \frac{\partial v_z(x,y,0)}{\partial x} \quad . \tag{63}$$

Since $\Delta v_z(x,y,0) = 0$, we learn that the difference between the values of the streamwise velocity at the surface of the wing and in the plane $z = 0$ is to second-order accuracy the same for the wing-fuselage configuration as for the isolated wing:

$$v_x(x,y,z_t) = v_x(x,y,0) + z_t \frac{\partial^2 z_t(x,y)}{\partial x^2} \quad .$$

We obtain thus from second-order theory

$$v_x(x,y,z_t) = v_{xw}^{(2)}(x,y,0) + \Delta v_x^{(2)}(x,y,0) + \Delta^* v_x(x,y,0) + z_t \frac{\partial^2 z_t(x,y)}{\partial x^2} \tag{64}$$

where $v_{xw}^{(2)}(x,y,0)$ is the velocity component for the isolated wing induced in $z = 0$ by $q_w^{(2)}(x,y)$, $\Delta v_x^{(2)}(x,y,0)$ is the interference velocity induced in $z = 0$ by the source distribution $q_f(x,\theta)$ on the fuselage, given by equation (50), and $\Delta^* v_x(x,y,0)$ is the velocity induced by the source distribution $\Delta q(x,y)$ given by equation (60).

Fig.6 shows that for small values of x/R the value of v_{xq} is changing rapidly when θ increases from $\theta = 0$ to $\theta = 10^{o}$ say, even though $\left(\frac{\partial v_{xq}}{\partial \theta}\right)_{\theta=0} = \frac{\partial v_{\theta}(x,\theta = 0)}{\partial x} = 0$, except for $x = 0$. With a 10 per cent thick wing and $c/R = 5$, the maximum value of $\theta_J(x)$ is 14.5^{o}. To learn how good an approximation to $\Delta v_x(x,y,z)$ is given by the first two terms of the Taylor's series, we have computed $\Delta v_x(x,\theta)$ at the fuselage using the $v_{xq}(x,\theta)$ given in Table 3. The results obtained with the first-order source distribution $q_w^{(1)}(x)$ of the wing are plotted in Fig.16. We note that the velocity decrement is over most of the chord somewhat larger for $z = z_t$ than for $z = 0$; at the maximum thickness position the change in Δv_x is about the same as the Δv_x produced by $q_w^{(2)}(x) - q_w^{(1)}$. The difference $\Delta v_x(\theta_J) - \Delta v_x(\theta = 0)$, though a third-order term can thus be of the same size as the second-order term $\Delta v_{xJ}(\theta = 0;\ \Delta q_w)$.

In Fig.17 we have plotted the total Δv_{xJ} computed at the surface of the wing from the source distribution for which the boundary condition is satisfied to second-order accuracy. The important feature is that the changes in Δv_x produced by the various second-order terms are, over most of the chord, of the same sign, namely that of the $\Delta v_{xJ}^{(1)}$ from first-order theory. Near the maximum thickness position, the second-order theory produces, in the wing-body junction, for $c/R = 5$, a 65 per cent larger velocity reduction than first-order theory; the corresponding value for $c/R = 2$ is 60 per cent.

This behaviour of the second-order corrections differs from that of the isolated wing. With the types of thickness distribution used in practice, the term $v_{xw}^{(1)}(x,z_t) - v_{xw}^{(1)}(x,0) = z_t \frac{d^2 z_t}{dx^2}$ is mostly a negative term, whilst $v_{xw}^{(2)}(x,0) - v_{xw}^{(1)}(x,0)$ is for most of the chord a positive term. As a consequence, the difference between the value from second-order theory, $v_{xw}^{(2)}(x,z_t)$ and the value from first-order theory $v_{xw}^{(1)}(x,0)$ is usually for much of the chord noticeably smaller than the second-order term $v_{xw}^{(2)}(x,0) - v_{xw}^{(1)}(x,0)$. This statement does of course not hold near the leading edge where the term $- z_t \frac{d^2 z_t}{dx^2}$ is large, and where the small perturbation theory needs a modification, as provided e.g. by the Riegels factor. We may quote that for the 10 per cent thick RAE 101 section at $x/c = 0.25$:

$$v_{xw}^{(1)}(x = 0.25,\ z = 0) = 0.1479$$

$$v_{xw}^{(2)}(x = 0.25,\ z = 0) - v_{xw}^{(1)}(x = 0.25,\ z = 0) = 0.0279$$

$$z_t\left(\frac{d^2 z_t}{dx^2}\right)_{x=0.25} = -0.0273 \ .$$

We have noted above that by approximating the source distribution on the fuselage $q_f(x,\theta)$ by a source distribution on the axis of the fuselage of strength $Q(x) = 4R\frac{dz_t}{dx}$ we obtain for the velocity decrement in the wing-body junction a larger value than the first-order term $-\Delta v_{xJ}^{(1)}$, see Fig.10. Since $\Delta v_{xJ}^{(1)}$ produces usually an underestimate of the actual interference effect, it is not surprising that for some configurations the axial source distribution has given a reasonably accurate estimate of the interference effect.

The pressure coefficient

$$c_p = 1 - (1 + v_x)^2 - v_y^2 - v_z^2$$

can be computed to second-order accuracy from

$$c_p = 1 - \left[1 + v_{xw}^{(2)} + \Delta v_x^{(2)}\right]^2 - (\Delta v_y^{(1)})^2 - \left[v_{zw}^{(2)} + \Delta v_z^{(2)}\right]^2$$

$$= 1 - \left[1 + \left(\frac{dz_t}{dx}\right)^2\right]\left[1 + v_{xw}^{(2)} + \Delta v_x^{(2)}\right]^2 - (\Delta v_y^{(1)})^2 \qquad (65)$$

except for the yet unknown term $(\Delta v_y^{(1)})^2$. However, in the wing-body junction the spanwise velocity is zero, and we may expect that for the combination of a fuselage with an unswept wing $(\Delta v_y^{(1)})^2$ is sufficiently small everywhere that we may neglect it.

3.3 Pressure distribution on the fuselage

To obtain the pressure distribution on the fuselage to first-order accuracy, we compute the streamwise perturbation velocity, v_x, induced by the sources in the wing plane and by the sources on the fuselage, from the equation

$$v_x(x,\theta) = \int_0^{c/R} q_w(x') \left\{ \frac{\frac{x}{R} - \frac{x'}{R}}{2\pi\left[\left(\frac{x}{R} - \frac{x'}{R}\right)^2 + \sin^2\theta\right]} + \frac{v_{xq}\left(\frac{x}{R} - \frac{x'}{R},\ \theta\right)}{Q/R} \right\} d\left(\frac{x'}{R}\right) \qquad (66)$$

with $q_w(x')$ from equation (43). Values of $\frac{v_{xq}}{Q/R}$ are given in Table 3.

For a fuselage attached to wings with a 10 per cent thick RAE 101 section and values $c/R = 2$ and $c/R = 5$, we have plotted the streamwise velocity at the top of the fuselage in Figs.18 and 19. We have also plotted the velocity $v_{xw}^{(1)}(x, z = R)$ which occurs in the flow past the isolated wing at the normal distance $z = R$ from the wing plane, computed with the source distribution $q_w^{(1)}(x)$. The figures show how the fuselage reduces the perturbation velocity by straightening the streamlines past the isolated wing. The velocity v_x on the top of the fuselage is of course noticeably larger for the fuselage with $c/R = 5$ than for the fuselage with $c/R = 2$ (note the different scales in Figs.18 and 19) because the distance from the wing plane, measured with respect to the wing chord is smaller for the case $c/R = 5$.

Figs.18 and 19 give also the velocity v_x at the section $\theta = 45^\circ$ of the fuselage, together with the velocity $v_{xw}^{(1)}(x, z = R/\sqrt{2})$ of the flow past the isolated wing.

To derive the pressure distribution on the fuselage to second-order accuracy, one would compute $v_x(x,\theta)$ from equation (66) with the source strength $q_w^{(2)}(x)$ from equation (59). The effect of taking $q_w^{(2)}(x)$ instead of $q_w^{(1)}(x)$ is shown for $\theta = 45^\circ$ in Figs.18 and 19.

A further second-order term in $v_x(x,\theta)$ will arise from the source distribution $\Delta q(x,y)$ in the wing plane, given by equation (60). As stated above, the spanwise distribution of $\Delta v_z(x,y,z_t)$ and therefore the spanwise variation of the additional source distribution $\Delta q(x,y)$ is not yet known. An inaccurate assumption about the source distribution can be more misleading if one wants to compute the induced Δv_x at $z \neq 0$, than if one computes Δv_x for $z = 0$. We have therefore not yet made an estimate of this term Δv_x (which would correspond to Δv_{xJ}^* of equation (61)).

A second-order term in the pressure coefficient on the fuselage is produced by the circumferential velocity component $v_\theta(x,\theta)$. This can be computed from

$$v_\theta(x,\theta) = \int_0^{c/R} q_w(x') \left\{ \frac{\sin\theta\cos\theta}{2\pi\left[\left(\frac{x}{R} - \frac{x'}{R}\right)^2 + \sin^2\theta\right]} + \frac{v_{\theta q}\left(\frac{x}{R} - \frac{x'}{R}, \theta\right)}{Q/R} \right\} d\left(\frac{x'}{R}\right) \qquad (67)$$

Values of $\frac{v_{\theta q}}{Q/R}$ are given in Table 4. Due to properties of symmetry, v_θ vanishes for $\theta = 0$ and $\theta = 90^\circ$. For the wing-fuselage configurations considered in Figs.18 and 19, we have computed v_θ for $\theta = 45^\circ$, with $q_w(x)$ from equation (43); results are plotted in Fig.20.

4 CONCLUSIONS AND FURTHER WORK

The flow field past a single straight infinite source line crossing a circular cylindrical fuselage at right angles has been studied.

It was found that the boundary condition at the surface of the fuselage can be satisfied to a relatively high degree of accuracy by a source distribution $q(x,\theta)$ on the surface of the fuselage of the strength

$$q(x,\theta) = -2v_{nQ}(x,\theta) + \bar{v}_{nQ}(x) + \Delta\bar{q}(x) \qquad (68)$$

where $\Delta\bar{q}(x)$ satisfies the onedimensional integral equation

$$\Delta\bar{q}(x) = \int_{-\infty}^{\infty} [\bar{v}_{nQ}(x') - \bar{v}_{nQ}(x) - \Delta\bar{q}(x') + \bar{\Delta}q(x)] \frac{k}{4\pi} [K - E]\, dx' \qquad (69)$$

where K and E are the complete elliptic integrals of modulus

$$k^2 = \frac{4}{4 + (x - x')^2} .$$

It has been found (report to be published) that equations (68) and (69) give a good approximation to $q(x,\theta)$ also for a single swept source line in the presence of a fuselage when the source line is continued inside of the fuselage up to the axis as the plane image on an infinite reflection plate at the side of the fuselage. We may therefore expect that for a wing-fuselage combination with a finite wing of varying section shape a sufficiently accurate source distribution can also be found by solving the onedimensional integral equation (69) instead of solving the complete twodimensional integral equation.

The velocity components induced by the source distribution $q(x,\theta)$ have been computed in the wing plane and at the surface of the fuselage.

The tabulated results have been used to derive for some wing-fuselage configurations the interference effect according to first-order theory. It was shown that the streamwise perturbation velocity in the wing-body junction can be reduced by 10 to 20 per cent.

The second-order terms have also been evaluated. It is shown that the reduction of the streamwise perturbation velocity according to second-order theory may be noticeably larger than according to first-order theory; for the cases considered by about 60 per cent. This suggests that for wing-fuselage combinations it may become more important to include all second-order terms than for isolated wings. To do this accurately one requires not only the velocity components induced in the wing plane but also those at the surface of the wing, in particular the v_z - velocity which the source distribution $q(x,\theta)$ on the fuselage induces at $z \neq 0$ is required. These have not yet been computed away from the fuselage.

Appendix A

EVALUATION OF $\lim_{x\to 0} v_{xq}(x > 0,\ y = 1,0)$ AND OF $\lim_{\theta\to 0} v_{\theta q}(x = 0,\theta)$

To determine the limit of $v_{xq}(x > 0,\ y = 1,\ z = 0)$ as x tends through positive values to zero, we use equation (22) with equations (19), (1) and (29) and it follows that, for $Q = 1$,

$$\lim_{x\to 0} v_{xq}(x,y = 1,0) =$$

$$= \lim_{x\to 0} -\frac{1}{\pi^2} \int_{-\infty}^{\infty} \int_{0}^{\pi} \frac{\sin^2\theta}{x'^2 + \sin^2\theta} \frac{(x - x')d\theta dx'}{\sqrt{(x - x')^2 + 2(1 - \cos\theta)}^3}$$

$$= \lim_{x\to 0} -\frac{1}{\pi^2} \int_{-\infty}^{\infty} \int_{0}^{\delta} \frac{\theta^2}{x'^2 + \theta^2} \frac{(x - x')d\theta dx'}{\sqrt{(x - x')^2 + \theta^2}^3}$$

$$= \lim_{x\to 0} +\frac{1}{\pi^2} \int_{-\varepsilon}^{\varepsilon} \int_{0}^{\delta} \frac{x'^2}{x'^2 + \theta^2} \frac{(x - x')d\theta dx'}{\sqrt{(x - x')^2 + \theta^2}^3} \qquad \text{(A-1)}$$

where ε and δ are non-zero. Now for $(x - x')^2 > x'^2$

$$\int_0^{\delta} \frac{d\theta}{(x'^2 + \theta^2)\sqrt{(x - x')^2 + \theta^2}^3} = -\frac{\delta}{[(x - x')^2 - x'^2](x - x')^2\sqrt{(x - x')^2 + \delta^2}}$$

$$+ \frac{1}{|x'|\sqrt{(x - x')^2 - x'^2}^3} \tan^{-1} \frac{\delta\sqrt{(x-x')^2 - x'^2}}{|x'|\sqrt{(x - x')^2 + \delta^2}}$$

and for $(x - x')^2 < x'^2$

$$\int_0^{\delta} \frac{d\theta}{(x'^2 + \theta^2)\sqrt{(x - x')^2 + \theta^2}^3} =$$

$$= -\frac{\delta}{[(x - x')^2 - x'^2]^2 \; (x - x')^2\sqrt{(x - x')^2 + \delta^2}}$$

$$-\frac{1}{2x'\sqrt{x'^2 - (x - x')^2}^3} \log \frac{x'\sqrt{(x - x')^2 + \delta^2} + \delta\sqrt{x'^2 - (x - x')^2}}{x'\sqrt{(x - x')^2 + \delta^2} - \delta\sqrt{x'^2 - (x - x')^2}} \; .$$

We introduce the variable τ by the relation

$$x' = x(1 + \tau) \; ,$$

then $(x - x')^2 > x'^2$ for $-\frac{\varepsilon}{x} - 1 < \tau < -0.5$ and $(x - x')^2 < x'^2$ for $-0.5 < \tau < \frac{\varepsilon}{x} - 1$.

We can then write

$$\lim_{x \to 0} \pi^2 v_{xq} =$$

$$= \lim_{x \to 0} \left\{ -\int_{-\frac{\varepsilon}{x} - 1}^{-0.5} \left[\frac{+\delta(1 + \tau)^2}{\tau(1 + 2\tau)\sqrt{x^2\tau^2 + \delta^2}} + \frac{\tau|1 + \tau|}{\sqrt{-2\tau - 1}^3} \tan^{-1} \frac{\delta\sqrt{-2\tau - 1}}{|1+\tau|\sqrt{x^2\tau^2 + \delta^2}} \right] d\tau \right.$$

$$\left. - \int_{-0.5}^{\frac{\varepsilon}{x} - 1} \left[\frac{\delta(1 + \tau)^2}{\tau(1+2\tau)\sqrt{x^2\tau^2 + \delta^2}} - \frac{\tau(1 + \tau)}{2\sqrt{2\tau+1}^3} \log \frac{(1+\tau)\sqrt{x^2\tau^2+\delta^2}+\delta\sqrt{2\tau+1}}{(1+\tau)\sqrt{x^2\tau^2+\delta^2}-\delta\sqrt{2\tau+1}} \right] d\tau \right\}$$

We take the limit as x/δ tends to zero and obtain

$$\lim_{x\to 0} \pi^2 v_{xq}(x,y = 1,0)$$

$$= \int_{0.5}^{\infty} \left[\frac{-4\tau^2}{4\tau^2 - 1} + \frac{\tau|1-\tau|}{\sqrt{2\tau - 1}^3} \tan^{-1} \frac{\sqrt{2\tau - 1}}{|1-\tau|} + \frac{\tau(1+\tau)}{2\sqrt{2\tau + 1}^3} \log \frac{1 + \tau + \sqrt{2\tau + 1}}{1 + \tau - \sqrt{2\tau + 1}} \right] d\tau$$

$$+ \int_{0}^{0.5} \left[+ \frac{4\tau^2}{1 - 4\tau^2} - \frac{\tau(1-\tau)}{2\sqrt{1 - 2\tau}^3} \log \frac{1 - \tau + \sqrt{1 - 2\tau}}{1 - \tau - \sqrt{1 - 2\tau}} + \right.$$

$$\left. + \frac{\tau(1+\tau)}{2\sqrt{1 + 2\tau}^3} \log \frac{1 + \tau + \sqrt{1 + 2\tau}}{1 + \tau - \sqrt{1 + 2\tau}} \right] d\tau \quad . \quad \text{(A-2)}$$

These integrals can be determined numerically. For $\tau \to 0.5$ the integrand in both integrals tends to $\frac{11}{12} - \frac{3}{16\sqrt{2}} \log \frac{1.5 + \sqrt{2}}{1.5 - \sqrt{2}}$. When $\tau \to \infty$ the integrand in the first integral behaves as $\frac{8}{15} \frac{1}{\tau^2}$. When $\tau \to 1$ the integrand in the first integral tends to $\frac{4}{3} - \frac{1}{3\sqrt{3}} \log \frac{2 + \sqrt{3}}{2 - \sqrt{3}}$. We have computed the value

$$\lim_{x\to 0} v_{xq}(x,y = 1,0) = -0.05305 \quad .$$

From equation (39) we obtain

$$\lim_{\theta\to 0} v_{\theta q}(x = 0,\theta) = \lim_{\theta\to 0} \int_{-\infty}^{\infty} \int_{0}^{2\pi} \frac{q(x',\theta') \sin(\theta - \theta')d\theta'dx'}{4\pi \sqrt{x'^2 + 2[1 - \cos(\theta - \theta')]}^3}$$

$$= \lim_{\theta\to 0} -\frac{1}{\pi^2} \int_{0}^{\infty} \int_{0}^{2\pi} \frac{\sin^2 \theta' \sin(\theta - \theta')d\theta'dx'}{[x'^2 + \sin^2 \theta']\sqrt{x'^2 + 2[1 - \cos(\theta - \theta')]}^3}$$

$$= \lim_{\theta\to 0} -\frac{1}{\pi^2} \int_{0}^{\varepsilon} \int_{-\delta}^{\delta} \frac{\theta'^2(\theta - \theta')d\theta'dx'}{[x'^2 + \theta'^2]\sqrt{x'^2 + (\theta - \theta')^2}^3} .$$

We compare this relation with equation (A-1) and note that, except for the sign, the integrals are the same if we interchange x with θ and x' with θ'. It follows that

$$\lim_{\theta\to 0} v_{\theta q}(x = 0,\theta) = -\lim_{x\to 0} v_{xq}(x,\theta = 0)$$

$$= 0.05305.$$

Appendix B

EVALUATION OF $\lim_{x\to 0} \Delta v_{z\Gamma}(x > 0,\ y = 1,\ z = 0)$

When writing Ref.1, we had not devised a treatment of the limiting process similar to the one of Appendix A.

An unswept vortex line in the presence of a cylindrical fuselage induces in the plane through the vortex and the axis of the fuselage an additional downwash

$$-\Delta v_z(x,y=1,0) = \int_{-\infty}^{\infty}\int_{0}^{2\pi} \frac{q(x',\theta)}{4\pi} \frac{\sin\theta\, d\theta dx'}{\sqrt{(x-x')^2 + 2(1-\cos\theta)^3}} .$$

The only term of $q(x,\theta)$ which contributes to the limiting value of Δv_z as x tends to zero reads

$$q(x,\theta) = \frac{\Gamma}{\pi} \frac{x \sin\theta}{x^2 + \sin^2\theta}$$

so that for $\Gamma = 1$

$$\lim_{x\to 0} -\Delta v_z = \lim_{x\to 0} \frac{1}{2\pi^2} \int_{-\infty}^{\infty}\int_{0}^{\pi} \frac{x' \sin^2\theta\, d\theta dx'}{(x'^2 + \sin^2\theta)\sqrt{(x-x')^2 + 2(1-\cos\theta)^3}} =$$

$$= \lim_{x\to 0} \frac{1}{2\pi^2} \int_{-\infty}^{\infty}\int_{0}^{\delta} \frac{x'\theta^2 d\theta dx'}{(x'^2 + \theta^2)\sqrt{(x-x')^2 + \theta^2}^3}$$

$$= \lim_{x\to 0}\left[\frac{1}{2\pi^2} \int_{-\infty}^{\infty}\int_{0}^{\pi} \left[\frac{x'}{x'^2+\theta^2} - \frac{x}{x^2+\theta^2}\right] \frac{\theta^2 d\theta dx'}{\sqrt{(x-x')^2+\theta^2}^3}\right.$$

$$\left. + \frac{x}{2\pi^2} \int_{0}^{\delta} \frac{\theta^2 d\theta}{x^2+\theta^2} \int_{-\infty}^{\infty} \frac{dx'}{\sqrt{(x-x')^2+\theta^2}^3}\right]$$

Now

$$\lim_{x\to 0} \frac{x}{2\pi^2} \int_0^{\delta} \frac{\theta^2 d\theta}{x^2+\theta^2} \int_{-\infty}^{\infty} \frac{dx'}{\sqrt{(x-x')^2+\theta^2}^3} = \frac{x}{2\pi^2} \int_0^{\delta} \frac{2d\theta}{x^2+\theta^2} =$$

$$= \lim_{x/\delta\to 0} \frac{1}{\pi^2} \tan^{-1}\frac{\delta}{x} = \frac{1}{2\pi} \quad .$$

After we have performed the integration with respect to θ, have introduced the variable τ by $x' = x(1+\tau)$ and taken the limit $\frac{x}{\delta} \to 0$, we obtain

$$\lim_{x\to 0} \frac{1}{2\pi^2} \int_{-\infty}^{\infty} \int_0^{\delta} \left[\frac{x'}{x'^2+\theta^2} - \frac{x}{x^2+\theta^2}\right] \frac{\theta^2 d\theta dx'}{\sqrt{(x-x')^2+\theta^2}^3} =$$

$$= -\frac{1}{2\pi^2} \left\{ \int_{-\infty}^{-0.5} \left[\frac{1+\tau}{1+2\tau} + \frac{(1+\tau)^2}{\sqrt{-2\tau-1}^3} \tan^{-1}\frac{\sqrt{-2\tau-1}}{1+\tau}\right] d\tau \right.$$

$$+ \int_{-0.5}^{\infty} \left[\frac{1+\tau}{1+2\tau} - \frac{(1+\tau)^2}{2\sqrt{1+2\tau}^3} \log\frac{1+\tau+\sqrt{1+2\tau}}{1+\tau-\sqrt{1+2\tau}}\right] d\tau$$

$$+ 2\int_1^{\infty} \left[\frac{1}{\tau^2-1} - \frac{1}{\sqrt{\tau^2-1}^3} \tan^{-1}\sqrt{\tau^2-1}\right] d\tau$$

$$\left. + 2\int_0^{+1} \left[\frac{1}{\tau^2-1} + \frac{1}{2\sqrt{1-\tau^2}^3} \log\frac{1+\sqrt{1-\tau^2}}{1-\sqrt{1-\tau^2}}\right] d\tau \right\} .$$

We have evaluated the integrals numerically and obtained the result:

$$\lim_{x\to 0} - \Delta v_z(x > 0, y = 1, 0) = \frac{1}{2\pi} - 0.05305$$

$$= 0.1061 \quad .$$

This value agrees well with the one derived in Ref.1 by graphical extrapolation from the values calculated for $x \neq 0$.

Appendix C

EVALUATION OF $\lim_{x\to 0} \int_{-\infty}^{\infty} \frac{[q(x',\theta = \kappa x) - q(x,\theta = \kappa x)]\, E(k)}{\pi(x - x')\sqrt{(x - x')^2 + 4}}\, dx'$

The terms $\bar{v}_n(x)$ and $\bar{\Delta q}(x)$ in $q(x,\theta)$ do not contribute to the limiting value of the integral. We have therefore to consider only

$$\lim_{x\to 0} I^* = \lim_{x\to 0} \int_{-\infty}^{\infty} \frac{-\left[\frac{\sin^2\theta}{x'^2 + \sin^2\theta} - \frac{\sin^2\theta}{x^2 + \sin^2\theta}\right] E(k)}{\pi^2(x - x')\sqrt{(x - x')^2 + 4}}\, dx'$$

$$= \lim_{x\to 0} - \frac{\sin^2\theta}{\pi^2(x^2 + \sin^2\theta)} \int_{-\infty}^{\infty} \frac{(x + x')\, E(k)\, dx'}{[x'^2 + \sin^2\theta]\sqrt{(x - x')^2 + 4}}$$

with $k^2 = \frac{4}{4 + (x - x')^2}$.

For small x

$$I^* \simeq - \frac{\sin^2\theta}{2\pi^2(x^2 + \sin^2\theta)} \int_{-\varepsilon}^{\varepsilon} \frac{(x + x')dx'}{[x'^2 + \sin^2\theta]}$$

$$\simeq - \frac{\sin^2\theta}{2\pi^2(x^2 + \sin^2\theta)} \frac{2x}{\sin\theta} \tan^{-1}\left(\frac{\varepsilon}{\sin\theta}\right)$$

where $\varepsilon >> x$.

With $\theta = \kappa x$, we obtain thus

$$\lim_{x\to 0} I^* = - \frac{\kappa}{2\pi(1 + \kappa^2)}$$

$|\lim I^*|$ has the maximum value $\frac{1}{4\pi}$ for $\kappa = 1$.

Table 1

VALUES OF $\sum_{n=1}^{6} \bar{K}^{(n)}(x)$

$$\bar{K}^{(n)}(x) = -\frac{1}{4\pi} \int_{-\infty}^{\infty} [\bar{K}^{(n-1)}(x') - \bar{K}^{(n-1)}(x)]\, k\,[K - E]\,dx'$$

where

$$k^2 = \frac{4}{4 + (x - x')^2}$$

$$\bar{K}^{(0)}(x) = -2\bar{v}_{nQ}(x)$$

x	$\sum_{n=1}^{6} \bar{K}^{(n)}(x)$	$\frac{1}{x}$	$x^2 \sum_{n=1}^{6} \bar{K}^{(n)}(x)$
0	-0.1305	1.00	0.0098
0.05	-0.1157	0.95	0.0124
0.1	-0.1021	0.9	0.0155
0.15	-0.0896	0.85	0.0189
0.2	-0.0781	0.8	0.0227
0.25	-0.0674	0.75	0.0269
0.3	-0.0576	0.7	0.0315
0.35	-0 0485	0.65	0.0365
0.4	-0.0403	0.6	0.0417
0.45	-0.0329	0.55	0.0470
0.5	-0.0261	0.5	0.0522
0.55	-0.0201	0.45	0.0567
0.6	-0.0147	0.4	0.0603
0.65	-0.0100	0.35	0.0622
0.7	-0.0058	0.3	0.0618
0.75	-0.0022	0.25	0.0587
0.8	0.0010	0.2	0.0527
0.85	0.0038	0.15	0.0439
0.9	0.0061	0.1	0.0322
0.95	0.0081	0.05	0.0172
1.0	0.0098	0	0

Table 2

STREAMWISE VELOCITY COMPONENT ON THE WING, $v_{xq}(x,y,z=0)$, INDUCED BY THE SOURCE DISTRIBUTION $q(x,\theta)$ ON THE FUSELAGE

x \ y	1.0	1.05	1.1	1.25	1.5	2.0
0	-0.0530	0	0	0	0	0
0.05	-0.0495	-0.0320	-0.0165	-0.0056	-0.0022	-0.0008
0.1	-0.0467	-0.0388	-0.0264	-0.0106	-0.0043	-0.0015
0.15	-0.0444	-0.0399	-0.0312	-0.0148	-0.0063	-0.0023
0.2	-0.0423	-0.0396	-0.0331	-0.0181	-0.0083	-0.0030
0.3	-0.0389	-0.0377	-0.0339	-0.0222	-0.0114	-0.0044
0.4	-0.0364	-0.0356	-0.0332	-0.0243	-0.0139	-0.0056
0.6	-0.0321	-0.0318	-0.0306	-0.0252	-0.0167	-0.0077
0.8	-0.0288	-0.0285	-0.0278	-0.0243	-0.0177	-0.0092
1.0	-0.0259	-0.0258	-0.0253	-0.0228	-0.0177	-0.0101
1.25	-0.0228	-0.0227	-0.0224	-0.0208	-0.0170	-0.0105
1.5	-0.0202	-0.0202	-0.0199	-0.0187	-0.0157	-0.0106
1.75	-0.0180	-0.0181	-0.0177	-0.0168	-0.0146	-0.0104
2.0	-0.0160	-0.0162	-0.0159	-0.0152	-0.0135	-0.0100
2.5	-0.0128	-0.0131	-0.0129	-0.0123	-0.0113	-0.0089
3.0	-0.0104	-0.0107	-0.0106	-0.0102	-0.0094	-0.0078
3.5	-0.0086	-0.0090	-0.0088	-0.0084	-0.0079	-0.0068
4.0	-0.0072	-0.0075	-0.0073	-0.0072	-0.0068	-0.0059
5.0	-0.0051	-0.0054	-0.0054	-0.0052	-0.0049	-0.0045
10.0	-0.0014	-0.0015	-0.0016	-0.0015	-0.0015	-0.0015

Table 3

STREAMWISE VELOCITY COMPONENT ON THE FUSELAGE, $v_{xq}(x,\theta)$, INDUCED BY THE SOURCE DISTRIBUTION $q(x,\theta)$ ON THE FUSELAGE

x \ δ	0	5°	10°	20°	30°	45°	60°	75°	90°
0	-0.0530	0	0	0	0	0	0	0	0
0.05	-0.0495	-0.0629	-0.0384	-0.0196	-0.0131	-0.0090	-0.0072	-0.0062	-0.0059
0.1	-0.0467	-0.0683	-0.0603	-0.0366	-0.0254	-0.0177	-0.0141	-0.0123	-0.0118
0.15	-0.0444	-0.0604	-0.0661	-0.0493	-0.0359	-0.0257	-0.0207	-0.0182	-0.0175
0.2	-0.0423	-0.0535	-0.0642	-0.0569	-0.0446	-0.0329	-0.0269	-0.0239	-0.0229
0.3	-0.0389	-0.0450	-0.0553	-0.0615	-0.0551	-0.0440	-0.0372	-0.0338	-0.0327
0.4	-0.0364	-0.0399	-0.0477	-0.0586	-0.0584	-0.0513	-0.0451	-0.0415	-0.0404
0.6	-0.0321	-0.0338	-0.0380	-0.0483	-0.0545	-0.0554	-0.0528	-0.0506	-0.0498
0.8	-0.0288	-0.0297	-0.0323	-0.0397	-0.0466	-0.0519	-0.0530	-0.0526	-0.0524
1.0	-0.0259	-0.0265	-0.0282	-0.0335	-0.0395	-0.0461	-0.0492	-0.0504	-0.0506
1.25	-0.0228	-0.0233	-0.0243	-0.0279	-0.0325	-0.0388	-0.0428	-0.0450	-0.0456
1.5	-0.0202	-0.0205	-0.0212	-0.0238	-0.0272	-0.0324	-0.0365	-0.0388	-0.0396
1.75	-0.0180	-0.0182	-0.0187	-0.0204	-0.0231	-0.0274	-0.0309	-0.0332	-0.0339
2.0	-0.0160	-0.0161	-0.0165	-0.0179	-0.0199	-0.0233	-0.0263	-0.0283	-0.0289
2.5	-0.0128	-0.0129	-0.0132	-0.0140	-0.0152	-0.0172	-0.0194	-0.0207	-0.0212
3.0	-0.0104	-0.0104	-0.0106	-0.0111	-0.0119	-0.0133	-0.0147	-0.0156	-0.0159
3.5	-0.0086	-0.0086	-0.0087	-0.0091	-0.0096	-0.0105	-0.0114	-0.0121	-0.0123
4.0	-0.0072	-0.0072	-0.0073	-0.0075	-0.0079	-0.0085	-0.0091	-0.0096	-0.0098
5.0	-0.0051	-0.0051	-0.0052	-0.0053	-0.0055	-0.0059	-0.0062	-0.0065	-0.0066
10.0	-0.0014	-0.0014	-0.0014	-0.0014	-0.0015	-0.0016	-0.0018	-0.0019	-0.0019

Table 4

CIRCUMFERENTIAL VELOCITY COMPONENT ON THE FUSELAGE, $v_{\theta q}(x,\theta)$, INDUCED BY THE SOURCE DISTRIBUTION $q(x,\theta)$ ON THE FUSELAGE

x \ θ	0	5°	10°	20°	30°	45°	60°	75°	90°
0	0.0530	0.0496	0.0464	0.0399	0.0337	0.0249	0.0164	0.0082	0
0.05	0	0.0652	0.0519	0.0414	0.0344	0.0252	0.0165	0.0082	0
0.1	0	0.0709	0.0618	0.0454	0.0363	0.0260	0.0169	0.0084	0
0.15	0	0.0620	0.0677	0.0502	0.0389	0.0273	0.0175	0.0086	0
0.2	0	0.0532	0.0672	0.0549	0.0422	0.0288	0.0183	0.0090	0
0.3	0	0.0387	0.0593	0.0596	0.0482	0.0326	0.0203	0.0098	0
0.4	0	0.0292	0.0493	0.0593	0.0514	0.0357	0.0224	0.0108	0
0.5	0	0.0231	0.0409	0.0556	0.0521	0.0381	0.0243	0.0118	0
0.6	0	0.0188	0.0344	0.0507	0.0509	0.0394	0.0256	0.0125	0
0.8	0	0.0133	0.0251	0.0407	0.0451	0.0388	0.0266	0.0133	0
1.0	0	0.0099	0.0190	0.0325	0.0383	0.0356	0.0257	0.0132	0
1.25	0	0.0072	0.0140	0.0248	0.0306	0.0304	0.0231	0.0122	0
1.5	0	0.0055	0.0107	0.0192	0.0243	0.0252	0.0198	0.0107	0
1.75	0	0.0043	0.0083	0.0152	0.0196	0.0208	0.0168	0.0092	0
2.0	0	0.0034	0.0066	0.0122	0.0158	0.0172	0.0141	0.0078	0
2.5	0	0.0022	0.0044	0.0082	0.0108	0.0120	0.0100	0.0056	0
3.0	0	0.0016	0.0031	0.0058	0.0077	0.0086	0.0073	0.0041	0
3.5	0	0.0012	0.0023	0.0043	0.0057	0.0065	0.0055	0.0031	0
4.0	0	0.0009	0.0018	0.0033	0.0044	0.0050	0.0042	0.0024	0
5.0	0	0.0006	0.0011	0.0021	0.0028	0.0032	0.0027	0.0016	0
10.0	0	0.0001	0.0003	0.0005	0.0007	0.0008	0.0007	0.0004	0

SYMBOLS

c	wing chord
$K^{(1)}(x,\theta)$	see equation (12)
$\bar{K}^{(\nu)}(x)$	see equation (18)
Q	strength of infinite source line
$q(x,\theta)$	strength of source distribution on the fuselage related to a single source line in the plane $z = 0$
$q^{(0)}(x,\theta)$	first approximation to $q(x,\theta)$, see equation (8)
$q^{(\nu)}(x,\theta)$	$(\nu + 1)$th approximation to $q(x,\theta)$
$\Delta q(x,\theta) = q(x,\theta) - q^{(0)}(x,\theta)$	
$\bar{q}(x)$	mean value of source strength $q(x,\theta)$ at a station x
$q_f(x,\theta)$	strength of source distribution on the fuselage related to the source distribution $q_w(x)$ in the plane $z = 0$
$q_w(x,y)$	source distribution in the wing plane representing the isolated wing
$q_w^{(1)}(x,y)$	source distribution in first-order theory
$q_w^{(2)}(x,y)$	source distribution in second-order theory
$\Delta q(x,y)$	interference term of source distribution in the plane $z = 0$, see equation (60)
R	radius of fuselage
x,y,z	rectangular coordinate system, x along the axis of the fuselage
x,r,θ	system of cylindrical coordinates
$z_t(x)$	section shape
V_0	free stream velocity, taken as unity
v_x, v_y, v_z	components of perturbation velocity
v_n	velocity component normal to the surface of the fuselage
$\bar{v}_n(x)$	mean value of $v_n(x,\theta)$
v_θ	circumferential velocity components at the surface of the fuselage
v_{xQ}, v_{zQ}, v_{nQ}, $v_{\theta Q}$	velocity components induced by the isolated source line
v_{xq}, v_{zq}, $v_{\theta q}$	velocity components induced by the source distribution $q(x,\theta)$ on the fuselage
v_{xw}	streamwise velocity component in the flow past the isolated wing
$v_{xw}^{(1)}$	v_{xw} according to first-order theory

SYMBOLS (Contd.)

$v_{xw}^{(2)}$	v_{xw} according to second-order theory
Δv_x, Δv_z	interference velocity components
Δv_{zJ}	Δv_z in the wing-body junction

REFERENCES

No.	Author	Title, etc.
1	J. Weber	Interference problems on wing-fuselage combinations. Part I: Lifting unswept wing attached to a cylindrical fuselage at zero incidence in midwing position. RAE Technical Report 69130 (ARC 31532) (1969)
2	D. Küchemann	Some remarks on the interference between a swept wing and a fuselage. RAE Technical Report 70093 (ARC 32307) (1970)
3	J. L. Hess A.M.O. Smith	Calculation of potential flow about arbitrary bodies. Progress in Aeron. Scs., Vol.8 (1967)
4	D. Küchemann J. Weber	The subsonic flow past swept wings at zero lift without and with body. ARC R & M 2908 (1953)
5	B. Thwaites (Ed.)	Incompressible Aerodynamics, Oxford, Clarendon Press (1960)

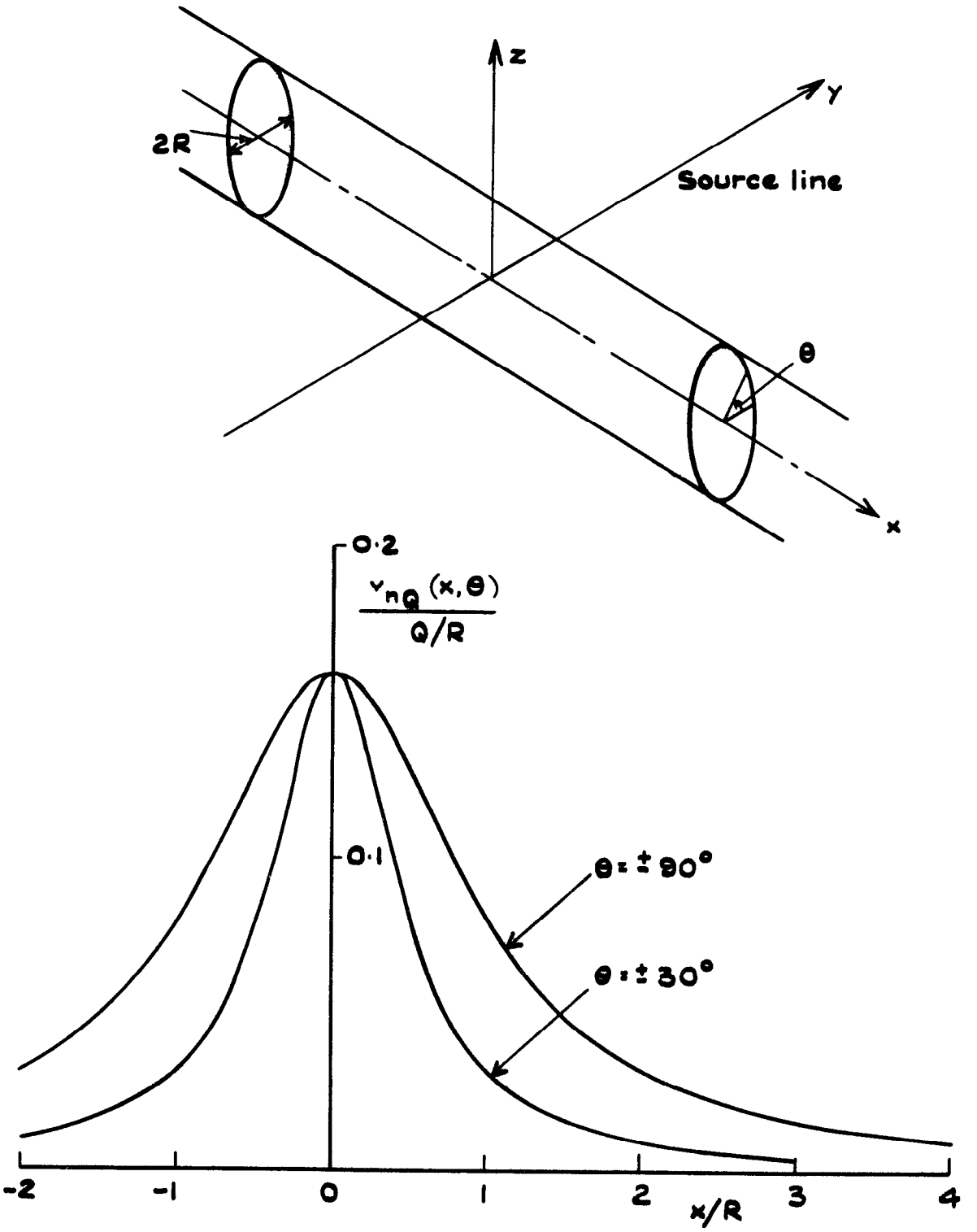

Fig.1 Normal velocity at the fuselage induced by a straight source line

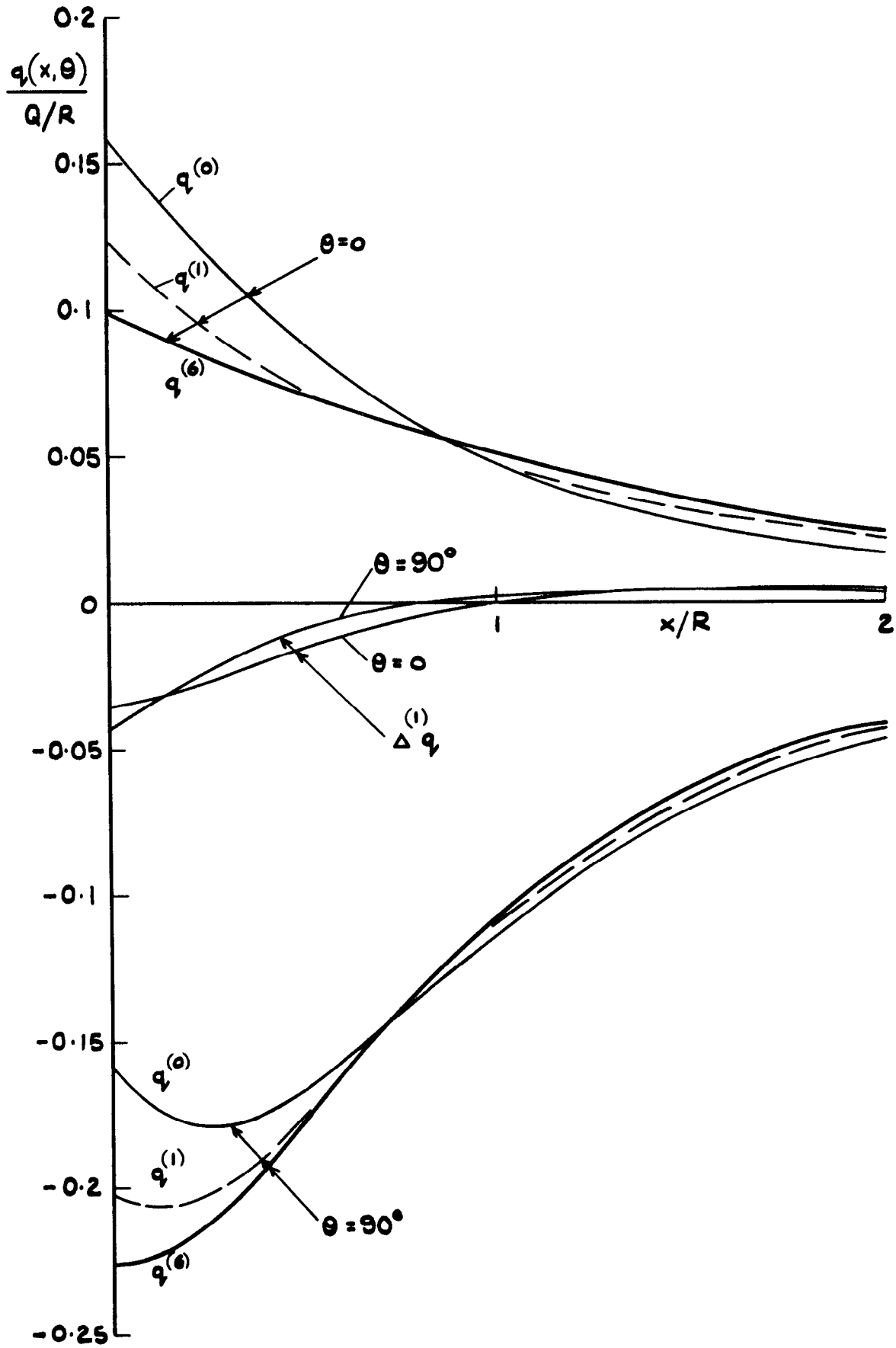

Fig. 2 Strength of source distribution on fuselage

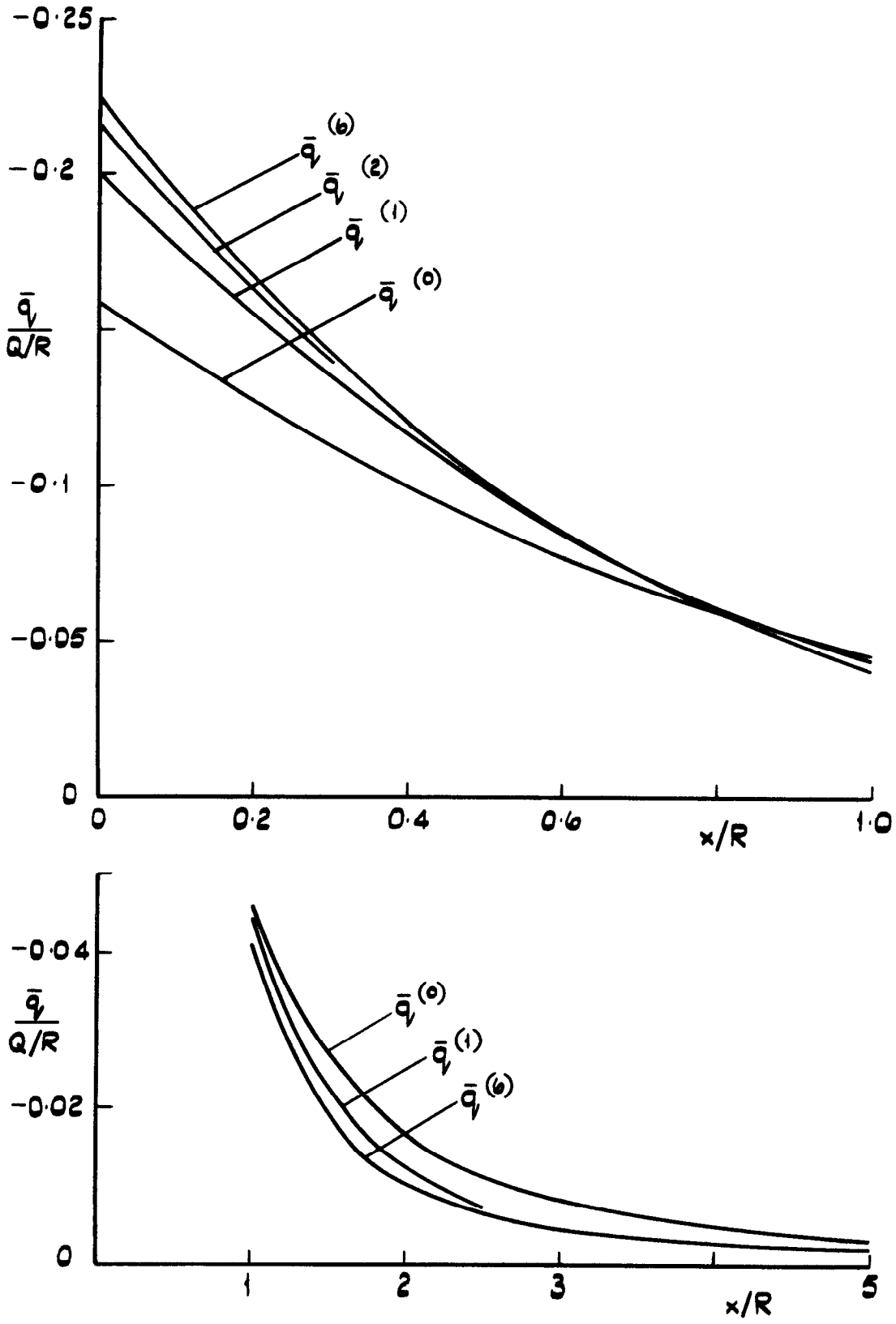

Fig.3 Average strength of source distribution on fuselage

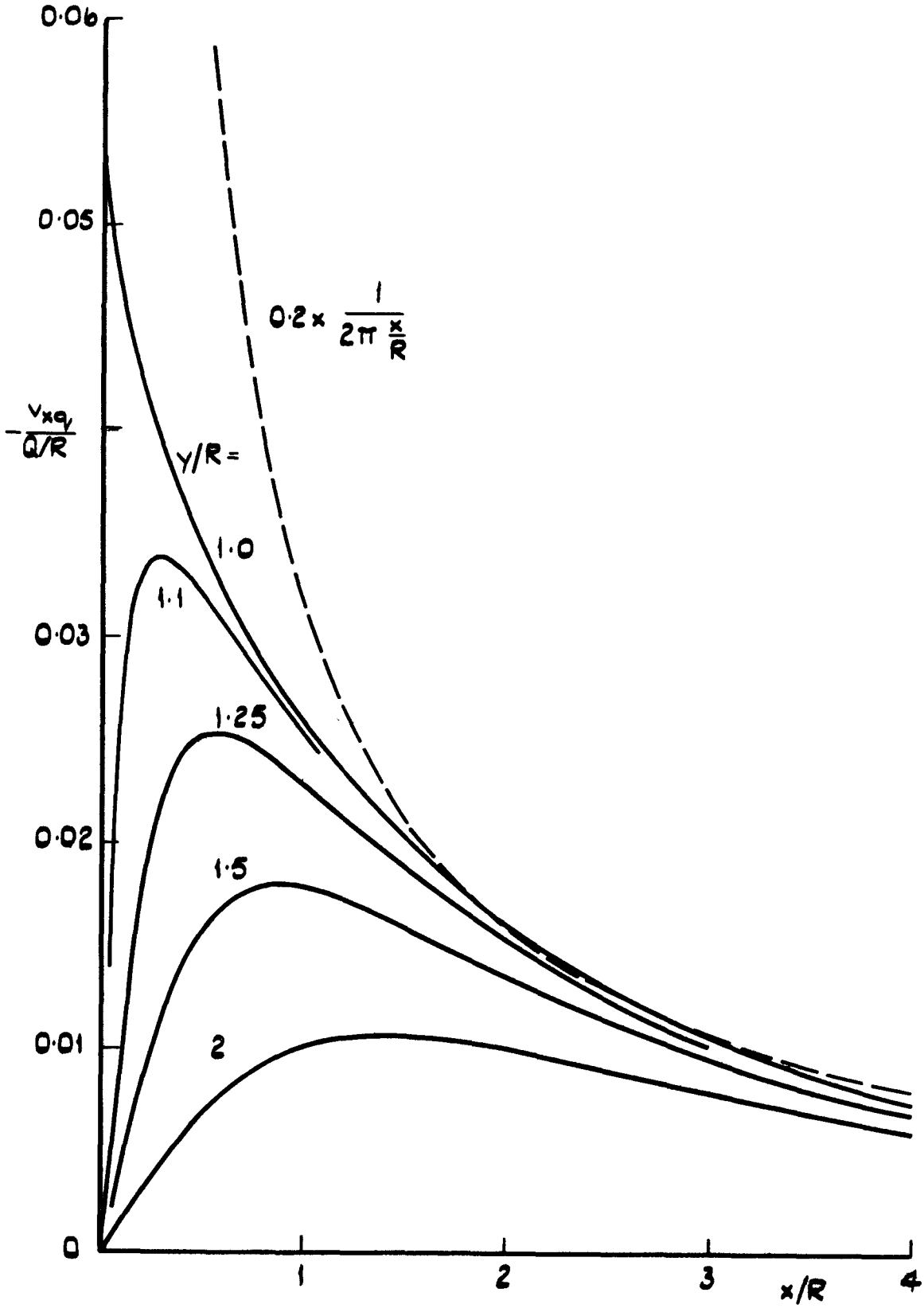

Fig.4 Additional streamwise velocity in the wing plane, z=O, induced by the source distribution on the fuselage

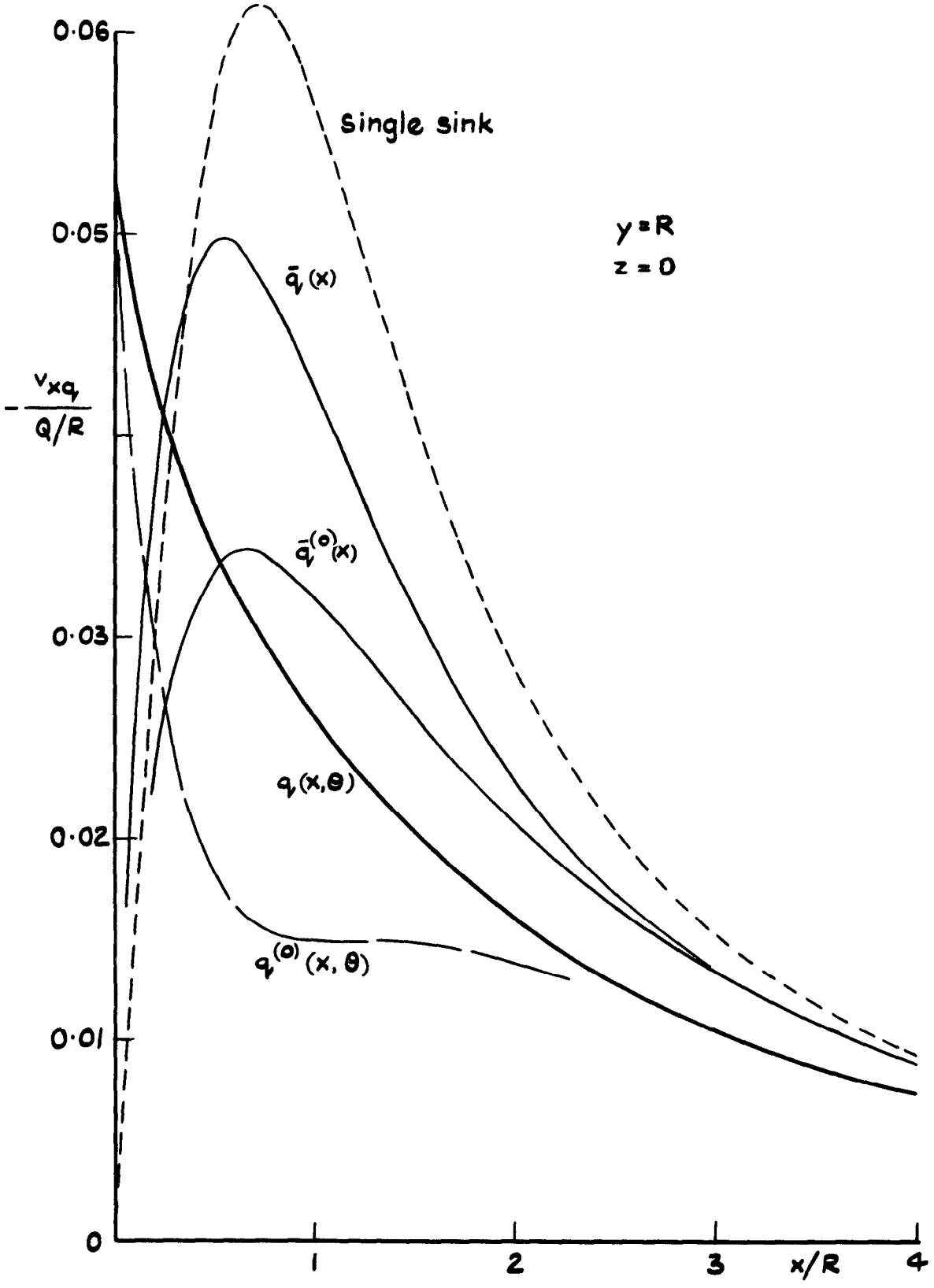

Fig. 5 Additional streamwise velocity in the wing-body junction

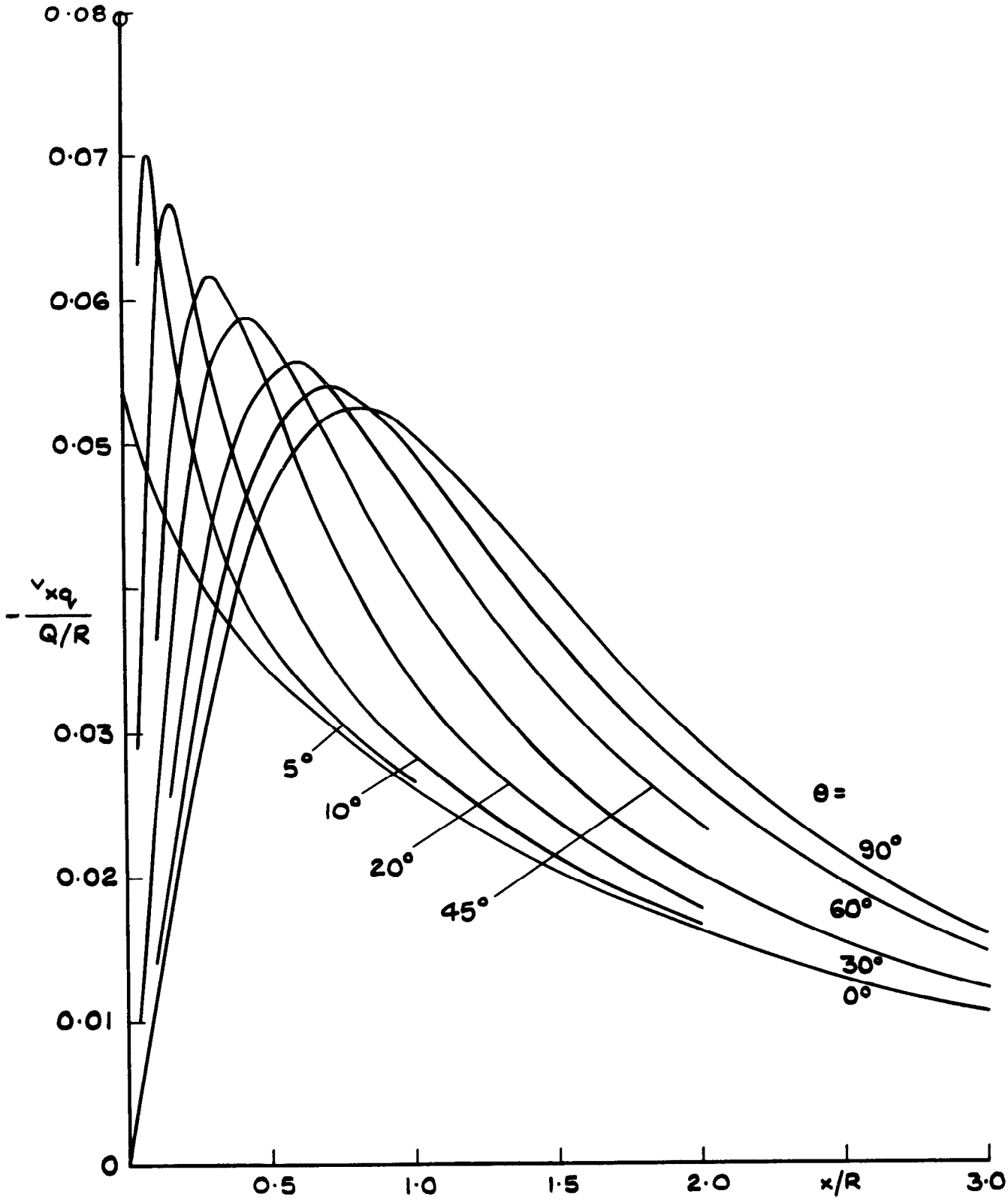

Fig. 6 Streamwise velocity on the fuselage due to source distribution on the fuselage

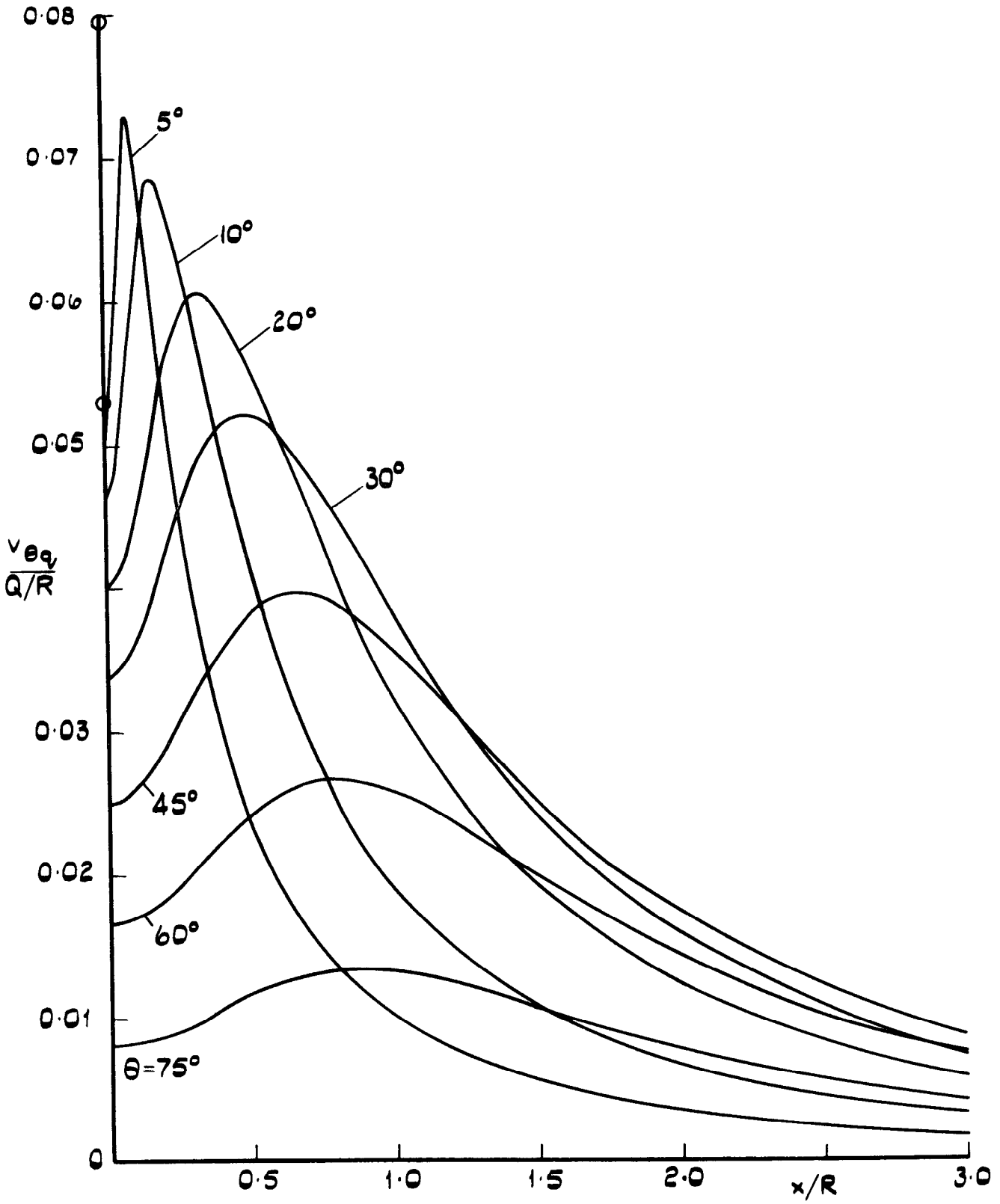

Fig.8 Circumferential velocity on the fuselage due to source distribution on the fuselage

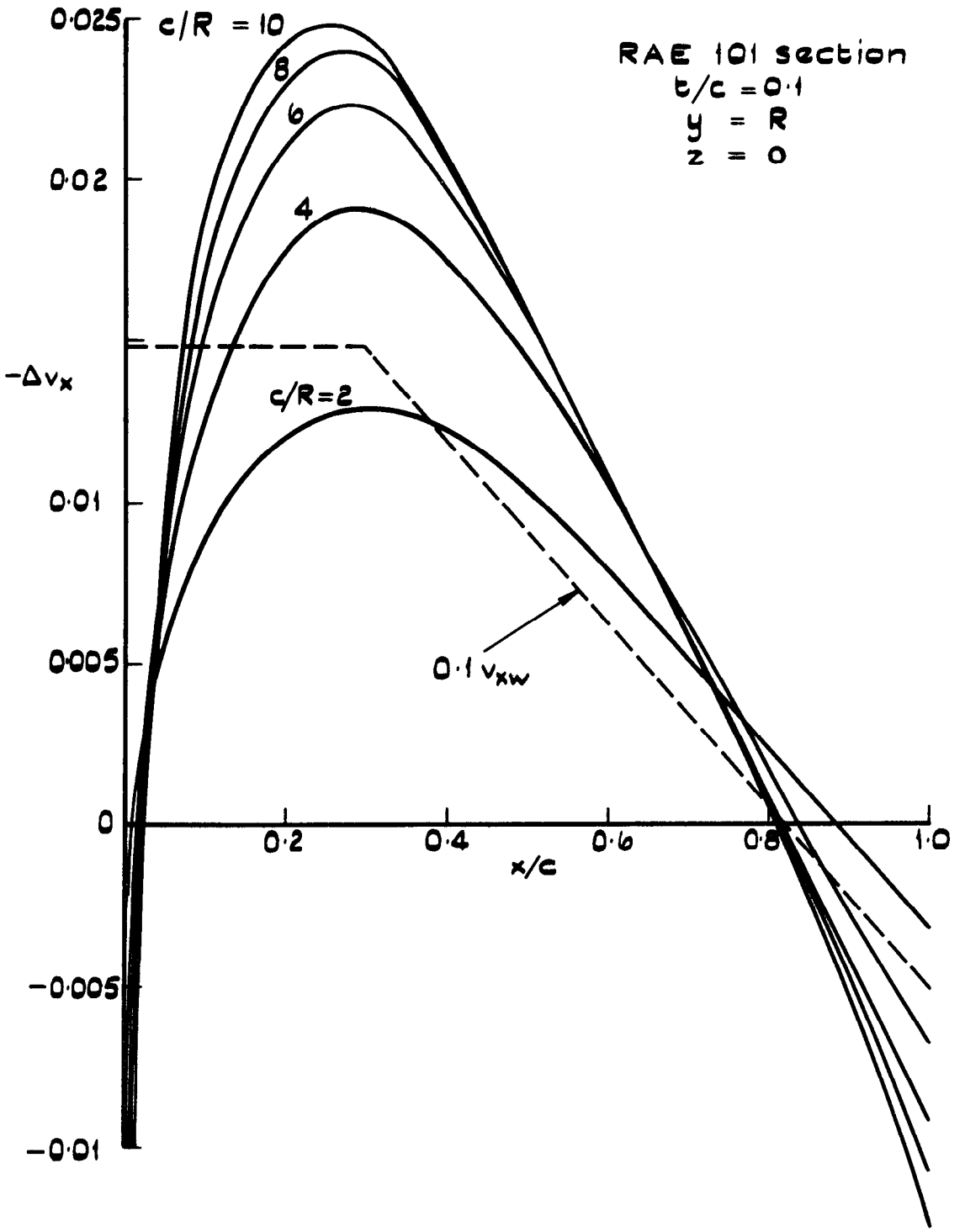

Fig.9 Interference velocity in the wing-body junction according to first-order theory

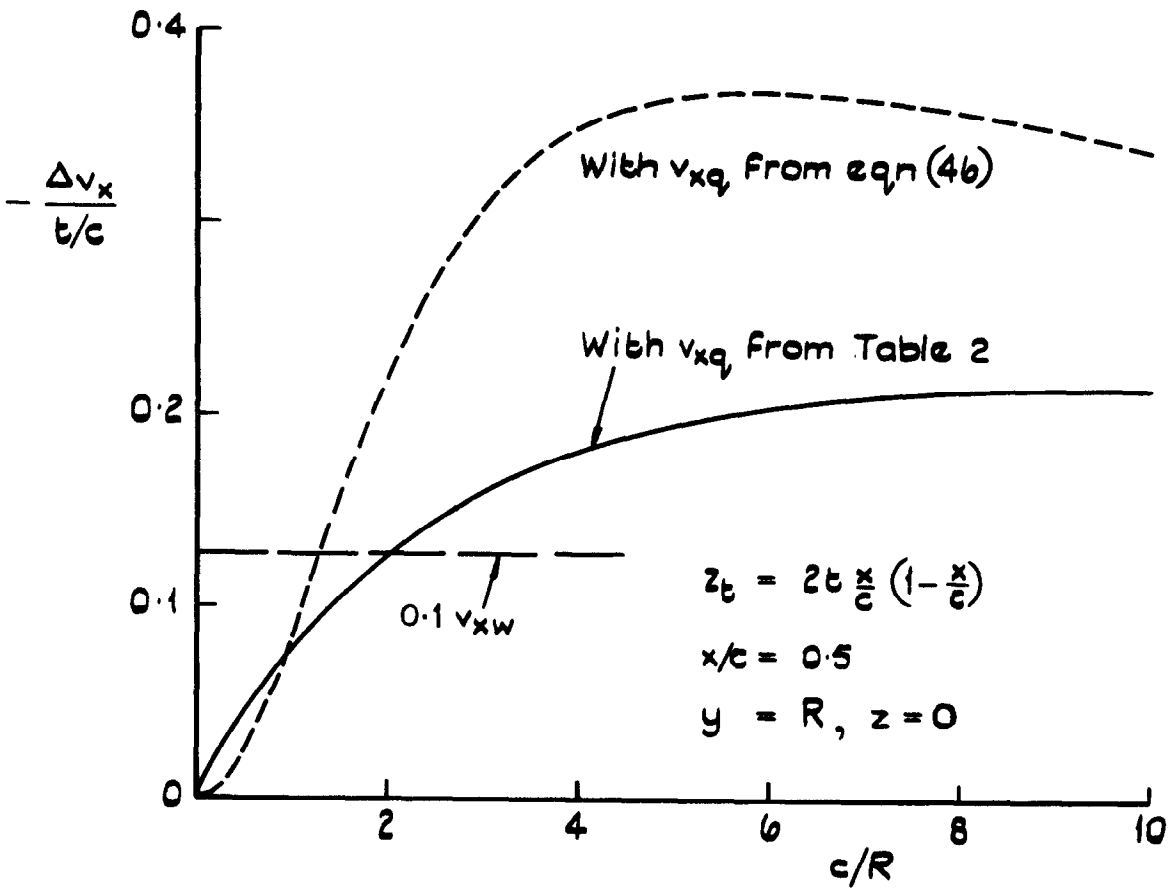

Fig.10 Velocity decrement at midchord of the wing-body junction for a wing with biconvex chordwise thickness distribution,

$$z_t = 2t\frac{x}{c}\left(1-\frac{x}{c}\right)$$

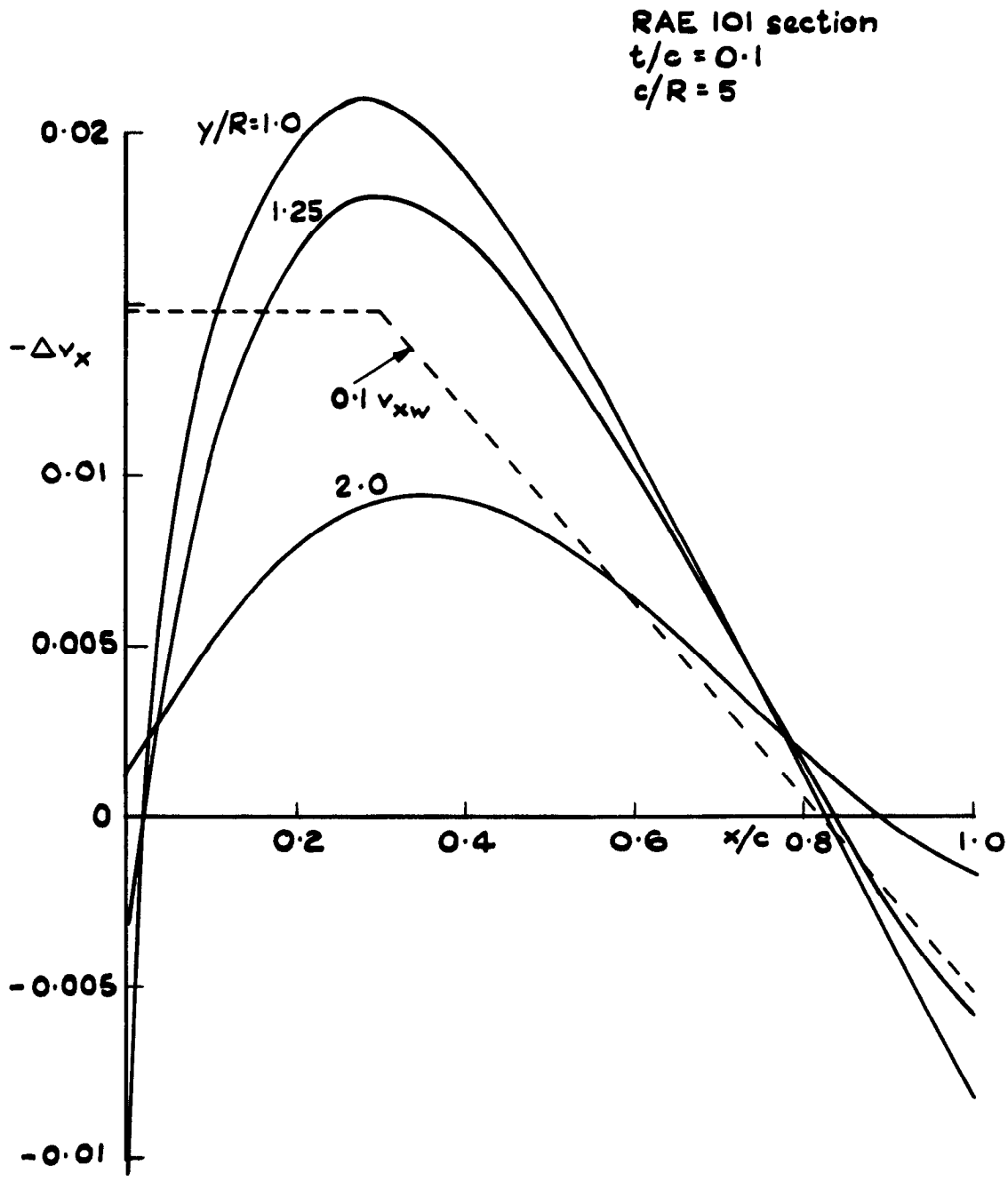

Fig. 11 Interference velocity in the plane of the wing

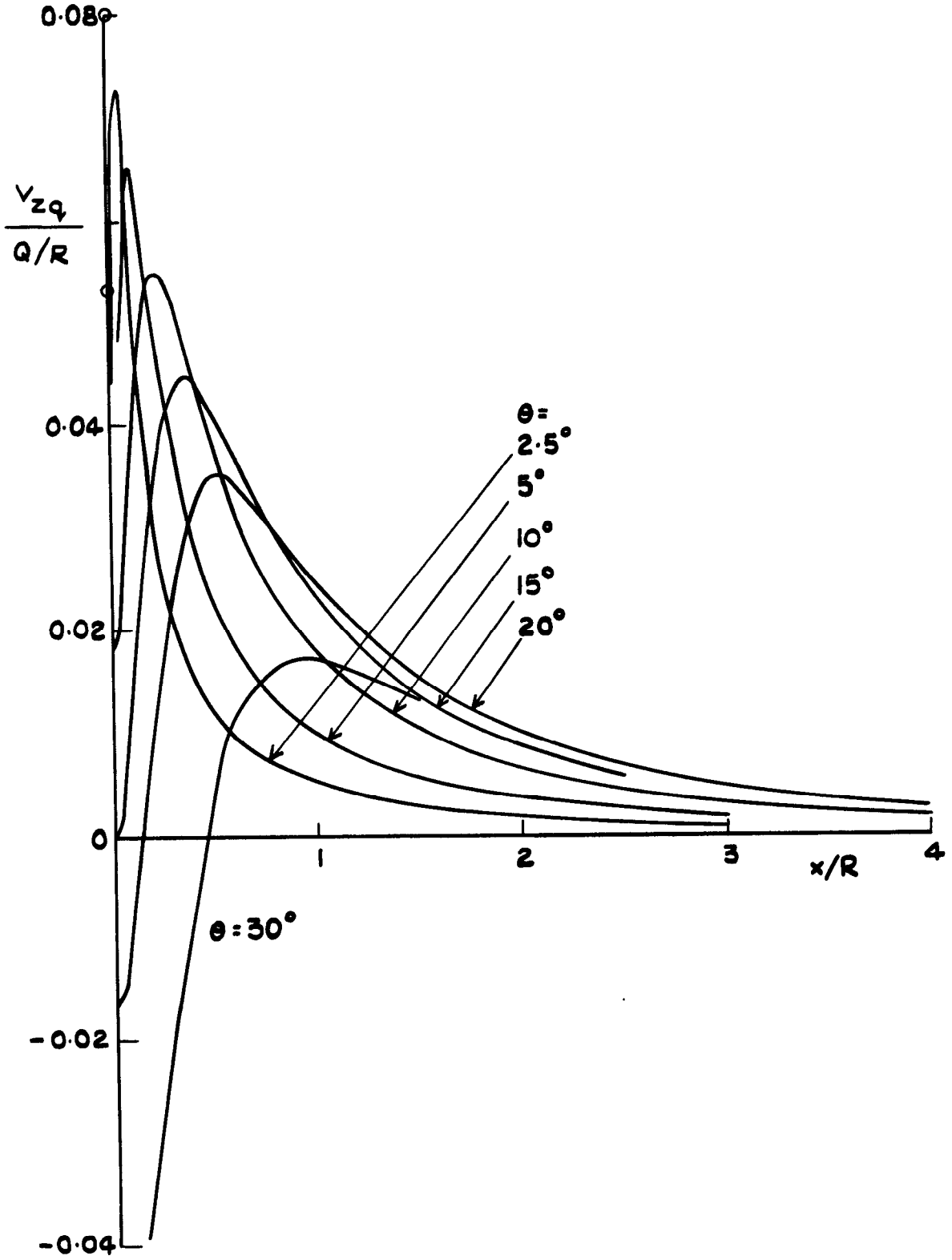

Fig. 12 v_z-velocity component on the fuselage due to the source distribution on the fuselage

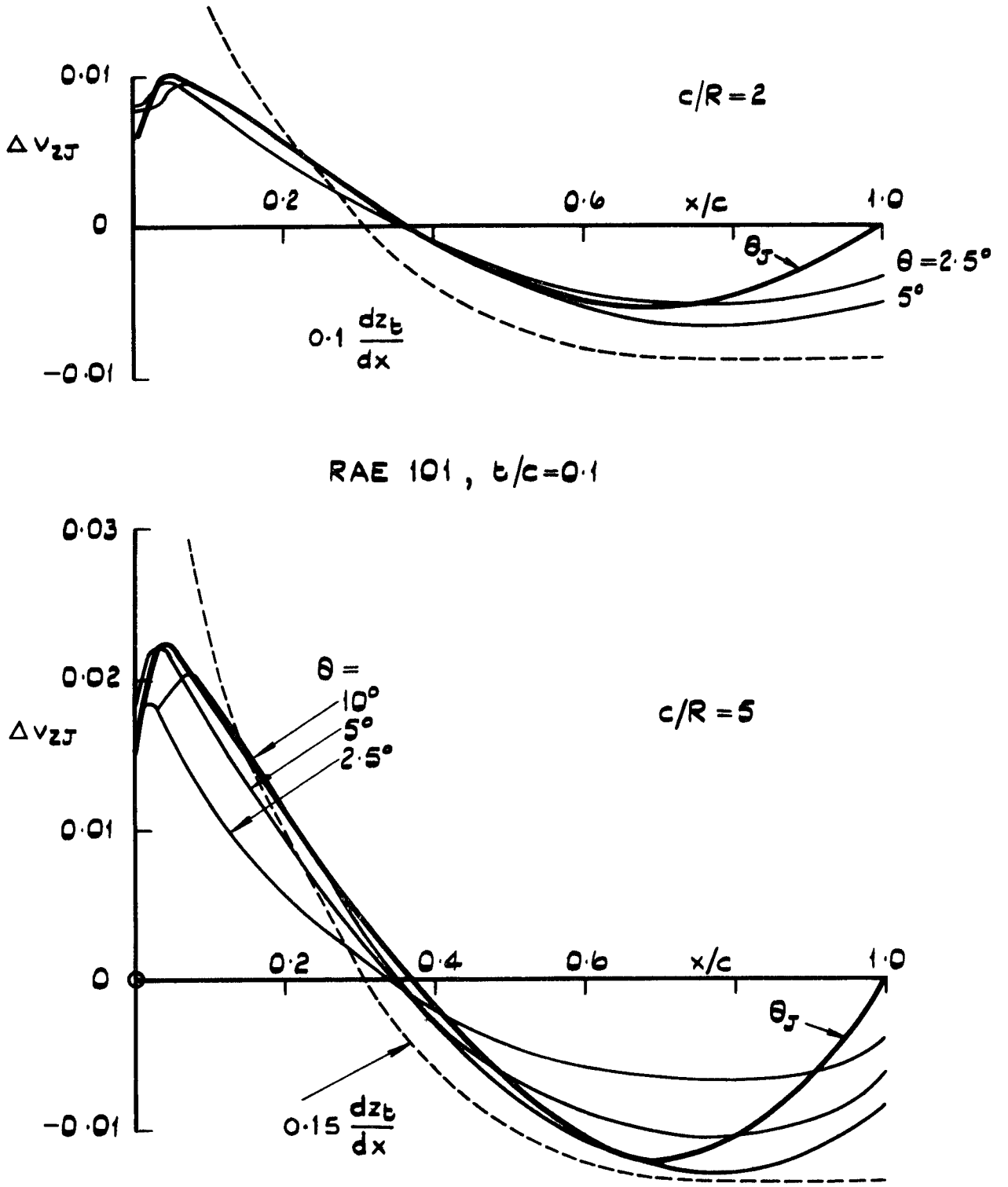

Fig.13 v_z – velocity component in the wing-body junction due to the source distribution on the fuselage

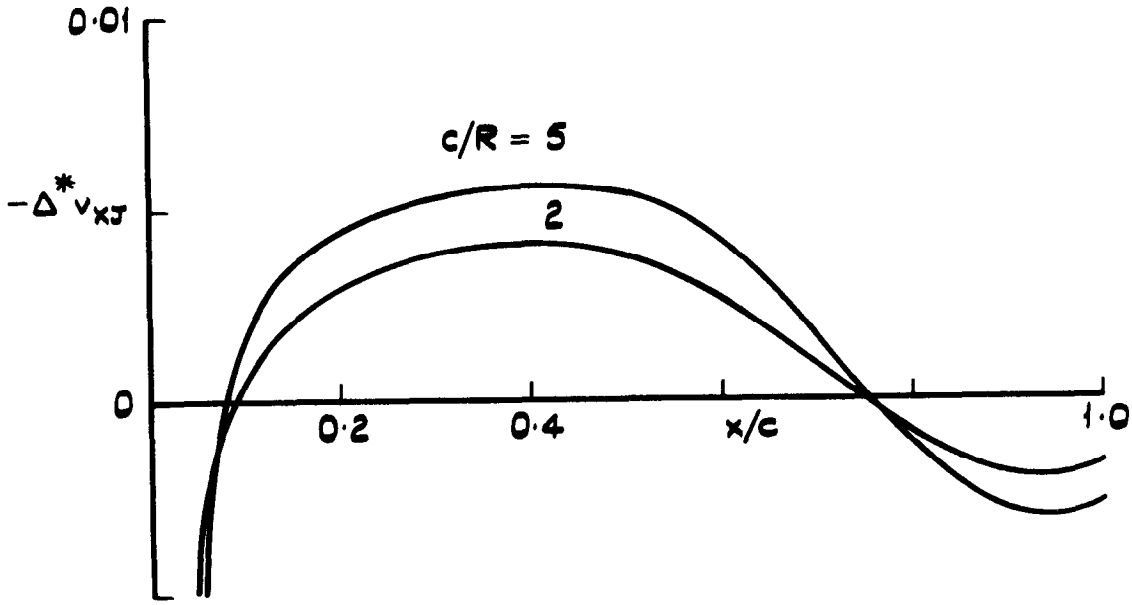

Fig.14 Velocity decrease according to eqn (61) with Δv_{zJ} from Fig.13

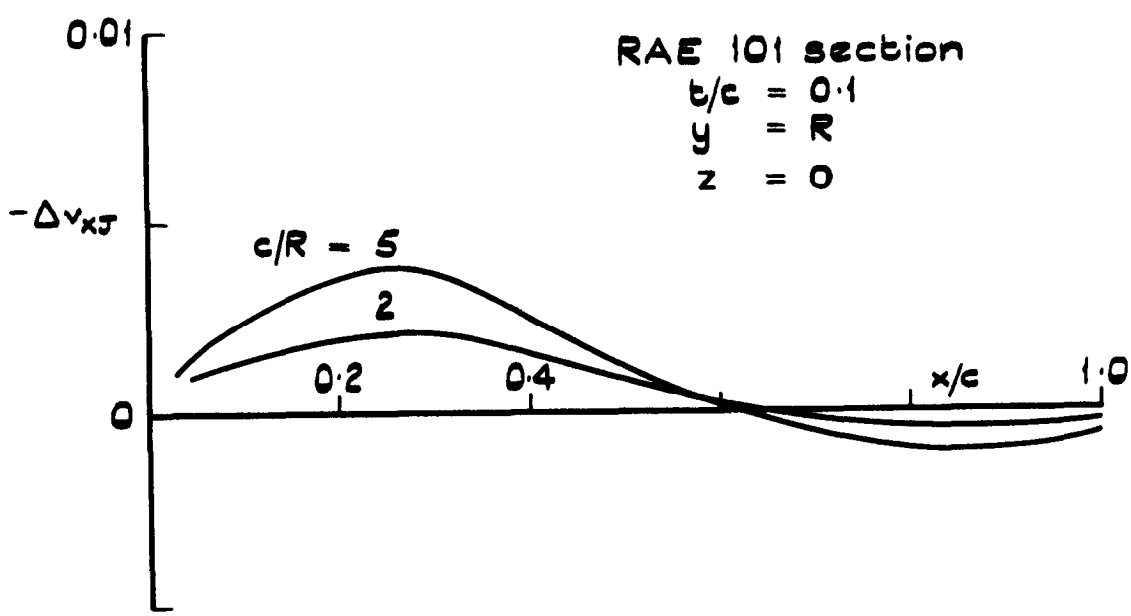

Fig.15 Change of interference velocity in the wing-body junction due to $q_w^{(2)}(x) - q_w^{(1)}(x)$

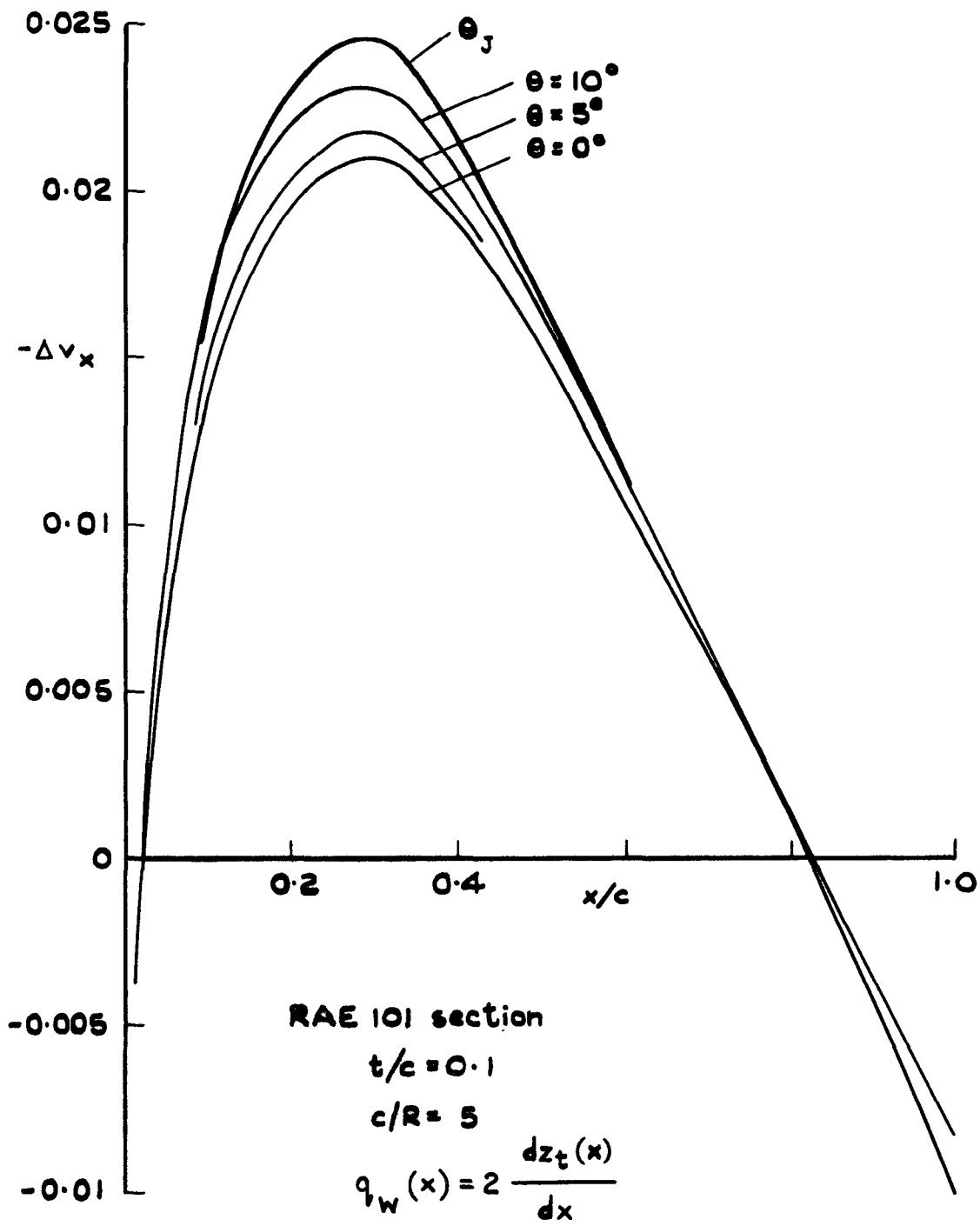

Fig.16 Streamwise velocity in the wing-body junction due to the source distribution on the fuselage

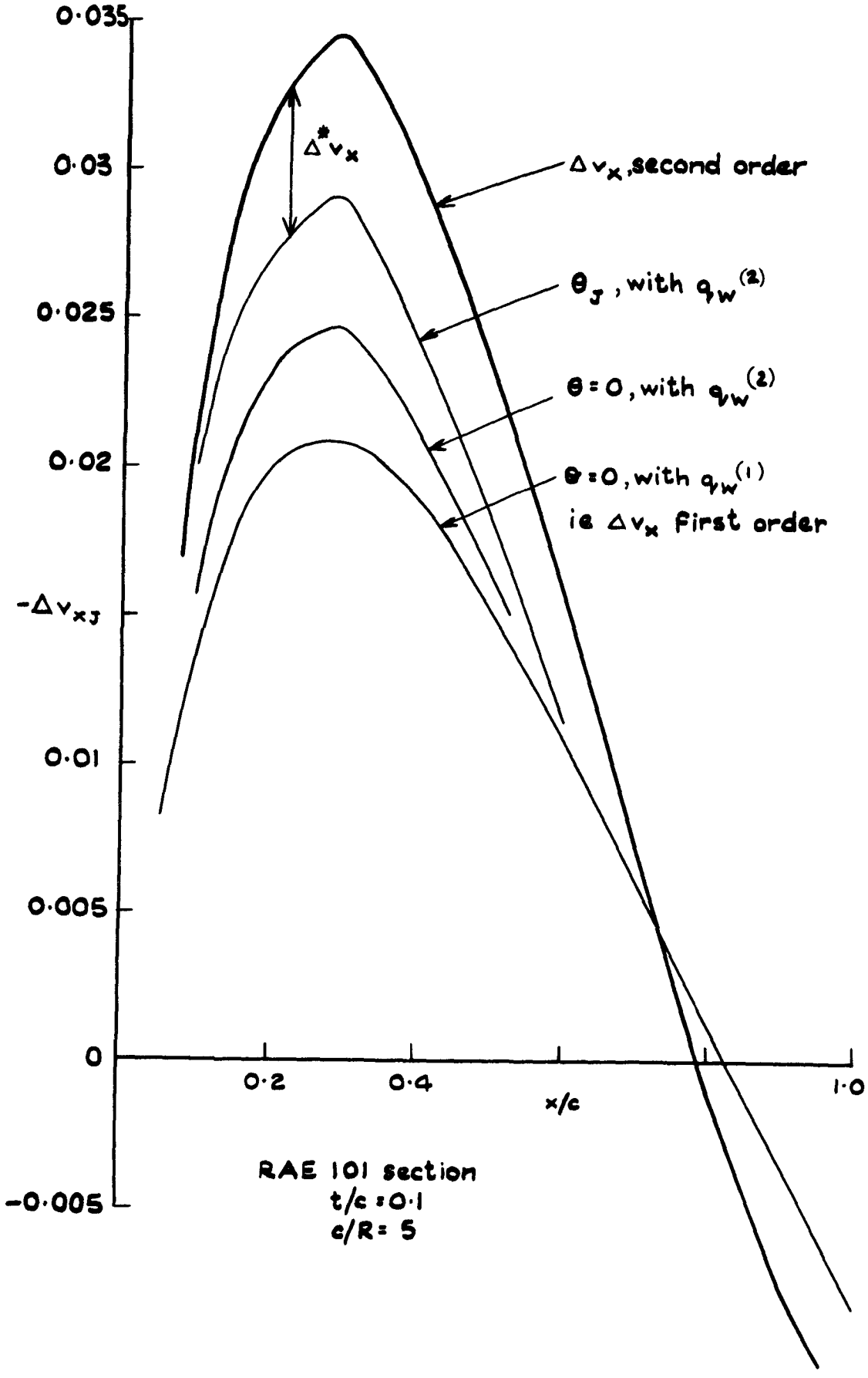

Fig. 17 Interference velocity in the wing-body junction

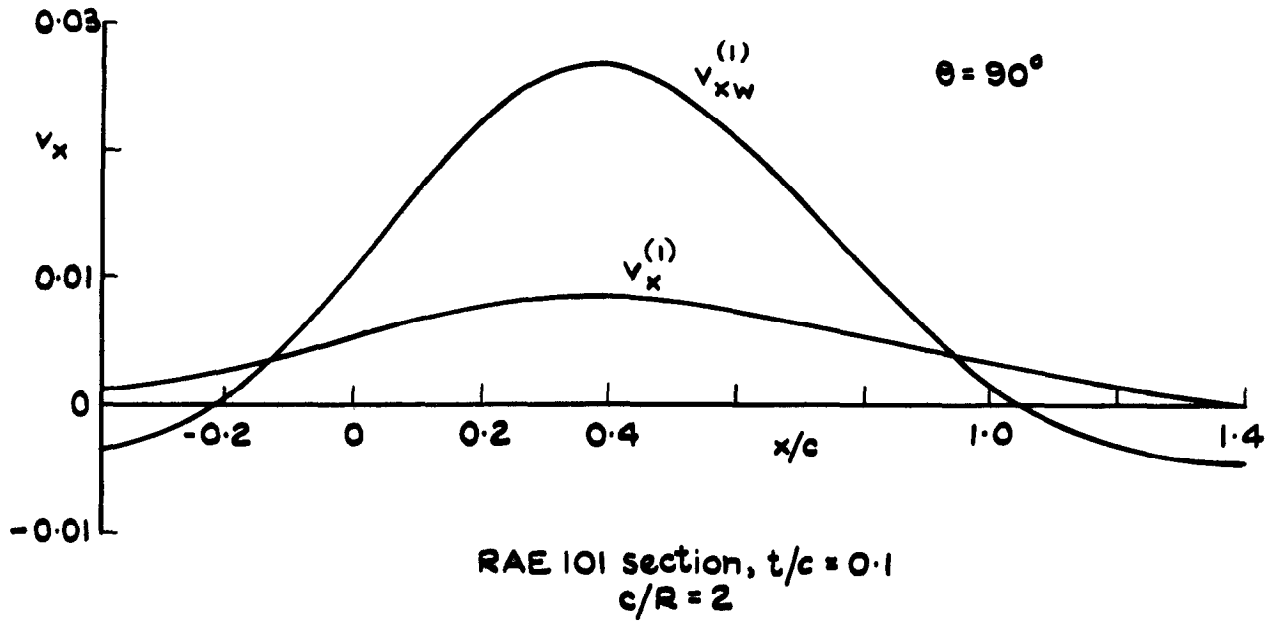

RAE 101 section, t/c = 0·1
c/R = 2

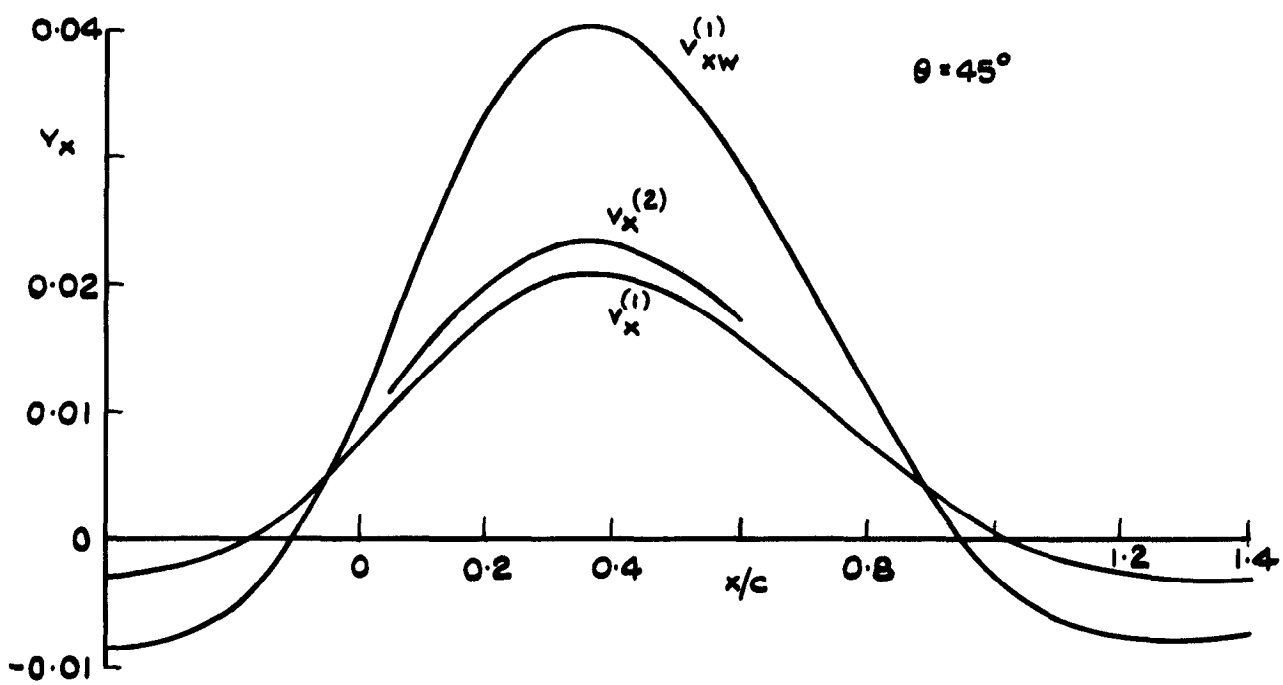

Fig. 18 Streamwise velocity component on the fuselage

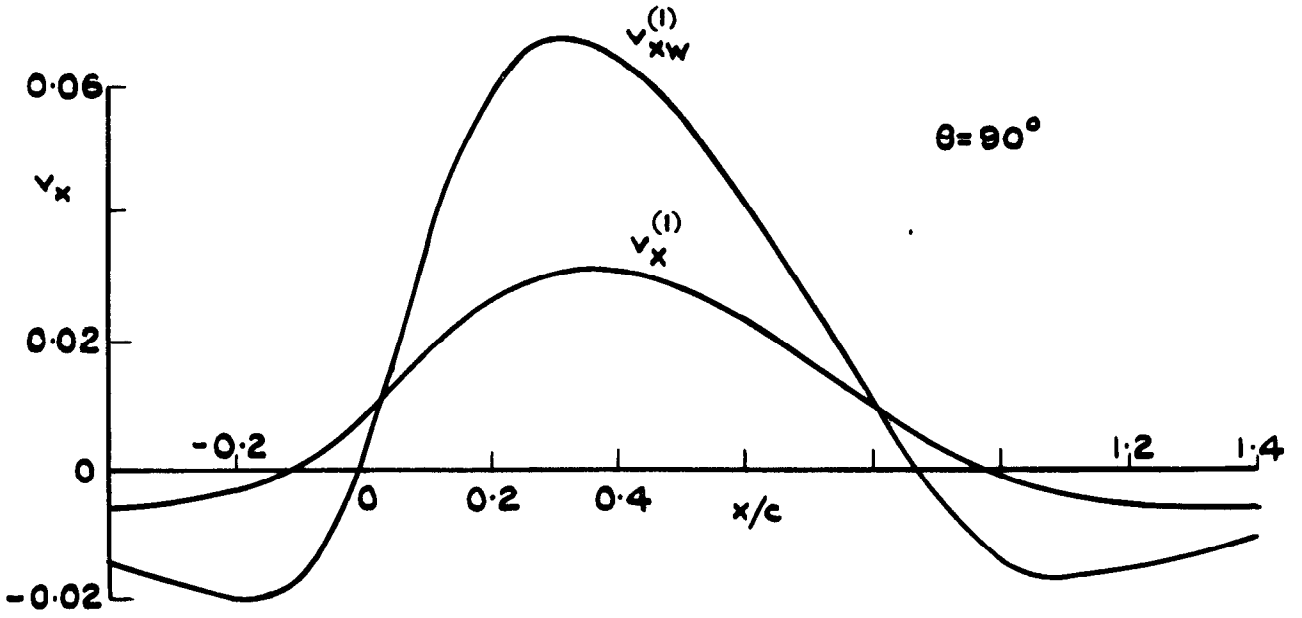

RAE 101 section, t/c = 0·1
c/R = 5

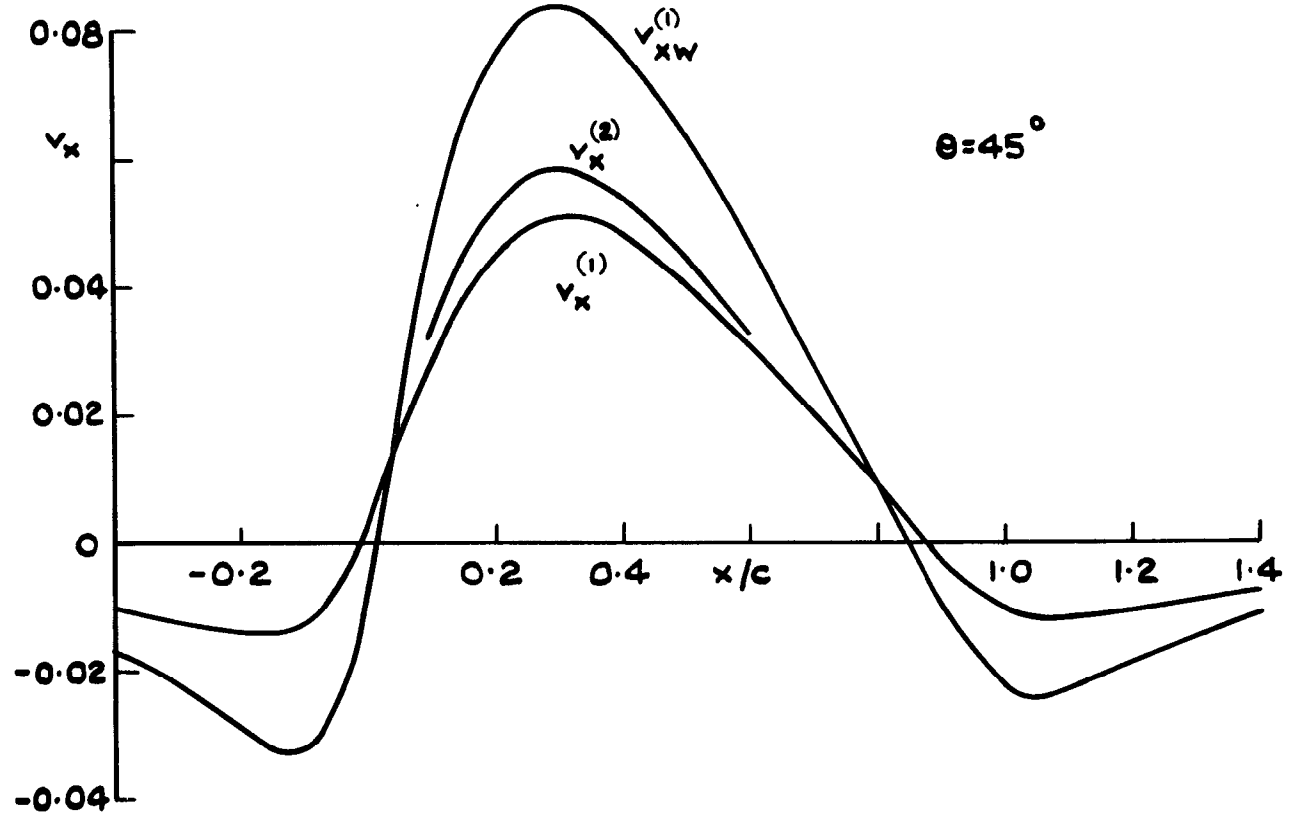

Fig. 19 Streamwise velocity component on the fuselage

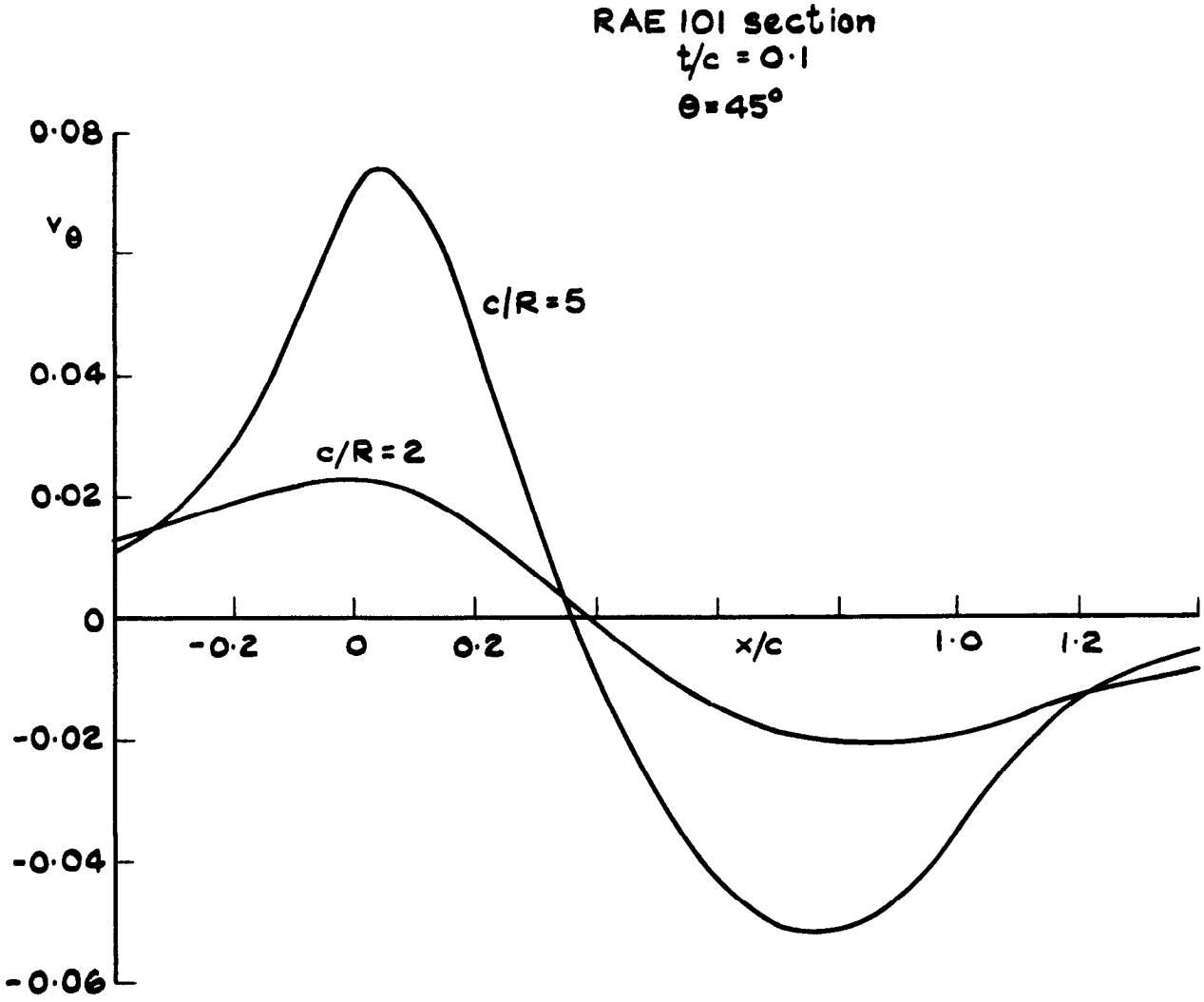

Fig. 20 Circumferential velocity component

Printed in England for Her Majesty's Stationery Office by the Royal Aircraft Establishment, Farnborough. Dd. 289030 K5 10/75.

ARC CP No 1332
August 1971

533.695.12
533 693.2
533.6.048.2 .
533.6 011.32

Weber, J.
Joyce, M. G

INTERFERENCE PROBLEMS ON WING-FUSELAGE COMBINATIONS. PART II: SYMMETRICAL UNSWEPT WING AT ZERO INCIDENCE ATTACHED TO A CYLINDRICAL FUSELAGE AT ZERO INCIDENCE IN MIDWING POSITION

The incompressible flow field past a single straight infinitely long source line which crosses a circular cylindrical fuselage at right angles has been studied In particular, the streamwise velocity component induced in the plane through the source line and the axis of the fuselage and the streamwise and circumferential velocity components induced on the surface of the fuselage have been determined numerically.

The results are used to determine the interference effect on the displacement flow past an unswept wing of infinite aspect ratio attached to a cylindrical fuselage It is shown how the interference effect varies with the ratio R/c between the body radius and the wing chord.

ARC CP No.1332
August 1971

533.695 12
533 693 2
533.6.048 2
533.6.011 32

Weber, J
Joyce, M. G

INTERFERENCE PROBLEMS ON WING-FUSELAGE COMBINATIONS PART II SYMMETRICAL UNSWEPT WING AT ZERO INCIDENCE ATTACHED TO A CYLINDRICAL FUSELAGE AT ZERO INCIDENCE IN MIDWING POSITION

The incompressible flow field past a single straight infinitely long source line which crosses a circular cylindrical fuselage at right angles has been studied In particular, the streamwise velocity component induced in the plane through the source line and the axis of the fuselage and the streamwise and circumferential velocity components induced on the surface of the fuselage have been determined numerically.

The results are used to determine the interference effect on the displacement flow past an unswept wing of infinite aspect ratio attached to a cylindrical fuselage. It is shown how the interference effect varies with the ratio R/c between the body radius and the wing chord.

Cut here

ARC CP No.1332
August 1971

533.695 12 :
533.693.2 :
533.6.048.2 .
533.6.011.32

Weber, J.
Joyce, M G.

INTERFERENCE PROBLEMS ON WING-FUSELAGE COMBINATIONS. PART II: SYMMETRICAL UNSWEPT WING AT ZERO INCIDENCE ATTACHED TO A CYLINDRICAL FUSELAGE AT ZERO INCIDENCE IN MIDWING POSITION

The incompressible flow field past a single straight infinitely long source line which crosses a circular cylindrical fuselage at right angles has been studied. In particular. the streamwise velocity component induced in the plane through the source line and the axis of the fuselage and the streamwise and circumferential velocity components induced on the surface of the fuselage have been determined numerically

The results are used to determine the interference effect on the displacement flow past an unswept wing of infinite aspect ratio attached to a cylindrical fuselage. It is shown how the interference effect varies with the ratio R/c between the body radius and the wing chord.

DETACHABLE ABSTRACT CARDS

ARC CP No 1332
August 1971

533.695.12
533 693.2
533.6 048.2
533.6.011.32

Weber, J.
Joyce, M. G.

INTERFERENCE PROBLEMS ON WING-FUSELAGE COMBINATIONS. PART II: SYMMETRICAL UNSWEPT WING AT ZERO INCIDENCE ATTACHED TO A CYLINDRICAL FUSELAGE AT ZERO INCIDENCE IN MIDWING POSITION

The incompressible flow field past a single straight infinitely long source line which crosses a circular cylindrical fuselage at right angles has been studied. In particular, the streamwise velocity component induced in the plane through the source line and the axis of the fuselage and the streamwise and circumferential velocity components induced on the surface of the fuselage have been determined numerically

The results are used to determine the interference effect on the displacement flow past an unswept wing of infinite aspect ratio attached to a cylindrical fuselage. It is shown how the interference effect varies with the ratio R/c between the body radius and the wing chord

Cut here

DETACHABLE ABSTRACT CARDS

C.P. No. 1332

1975

Published by
HER MAJESTY'S STATIONERY OFFICE

Government Bookshops
49 High Holborn, London WC1V 6HB
13a Castle Street, Edinburgh EH2 3AR
41 The Hayes, Cardiff CF1 1JW
Brazennose Street, Manchester M60 8AS
Southey House, Wine Street, Bristol BS1 2BQ
258 Broad Street, Birmingham B1 2HE
80 Chichester Street, Belfast BT1 4JY
Government Publications are also available through booksellers

C.P. No. 1332

ISBN 011 470942 4